

The Major Core Protein P4a (A10L Gene) of Vaccinia Virus Is Essential for Correct Assembly of Viral DNA into the Nucleoprotein Complex To Form Immature Viral Particles

RITVA HELJASVAARA,¹ DOLORES RODRÍGUEZ,¹ CRISTINA RISCO,² JOSÉ L. CARRASCOSA,² MARIANO ESTEBAN,^{1*} AND JUAN RAMÓN RODRÍGUEZ¹

Departments of Molecular and Cellular Biology¹ and Macromolecular Structure,² Centro Nacional de Biotecnología, Consejo Superior de Investigaciones Científicas, Campus Universidad Autónoma, Cantoblanco, 28049 Madrid, Spain

Received 28 July 2000/Accepted 2 April 2001

The vaccinia virus (VV) A10L gene codes for a major core protein, P4a. This polypeptide is synthesized at late times during viral infection and is proteolytically cleaved during virion assembly. To investigate the role of P4a in the virus life cycle and morphogenesis, we have generated an inducer-dependent conditional mutant (VVindA10L) in which expression of the A10L gene is under the control of the *Escherichia coli lacI* operator/repressor system. Repression of the A10L gene severely impairs virus growth, as observed by both the inability of the virus to form plaques and the 2-log reduction of viral yields. This defect can be partially overcome by addition of the inducer isopropyl-β-D-thiogalactopyranoside (IPTG). Synthesis of viral proteins other than P4a occurred, although early shutoff of host protein synthesis and expression of viral late polypeptides are clearly delayed, both in the absence and in the presence of IPTG, compared with cells infected with the parental virus. Viral DNA replication and concatemer resolution appeared to proceed normally in the absence of the A10L gene product. In cells infected with VVindA10L in the absence of the inducer virion assembly is blocked, as defined by electron microscopy. Numerous spherical immature viral particles that appear devoid of dense viroplasmic material together with highly electron-dense regular structures are abundant in VVindA10L-infected cells. These regularly spaced structures can be specifically labeled with anti-DNA antibodies as well as with a DNase-gold conjugate, indicating that they contain DNA. Some images suggest that these DNA structures enter into spherical immature viral particles. In this regard, although it has not been firmly established, it has been suggested that DNA uptake occurs after formation of spherical immature particles. Overall, our results showed that P4a and/or its cleaved products are essential for the correct assembly of the nucleoprotein complex within immature viral particles.

Vaccinia virus (VV), the prototype member of the *Poxviridae* family, is a large DNA virus whose replication and assembly occur entirely in the cytoplasm of the host cell, in particular areas termed viral factories or virosomes (33). The linear double-stranded DNA genome has a capacity to encode over 200 polypeptides (22), of which approximately 100 are incorporated into virus particles (14). The viral genes can be divided into three classes according to their temporally regulated expression. The early genes are transcribed prior to DNA replication, while the intermediate and late genes are transcribed only during or after replication of the viral genome (33).

Detailed information about VV morphogenesis has been obtained from studies by conventional electron microscopy (6, 7, 9, 21, 31, 32). Virus assembly begins within cytoplasmic viral factories with the formation of crescent-shaped membranes whose origin remains controversial. These membranes subsequently enclose granular material from the virosomes, forming spherical particles known as immature virions (IVs). The IVs undergo additional maturation events, transforming into brick-shaped structures where the envelope surrounds an electron-dense core structure containing viral DNA. These virions con-

stitute the first infectious form of VV, and they are referred to as intracellular mature virions (IMVs). A small portion of IMVs become wrapped by a membrane cisterna derived from the *trans*-Golgi network (50). These intracellular enveloped virions are released from the cell by fusion with the plasma membrane, a process whereby they lose the outermost membrane. The resulting extracellular enveloped virions are largely responsible for virus spread both in tissue culture and in animals (3, 37).

The complex morphological changes that occur during the transition from IV to IMV are poorly understood (33). After successful DNA replication and concatemer resolution (11, 30, 35), the viral genome is condensed and packaged as a nucleoprotein complex in the IVs (31, 32). Other events implicated in virus maturation include assembly and encapsidation of a multiprotein transcription complex (69), proteolytic processing of major structural proteins (25, 26, 34, 55, 56, 65), formation of a defined core (18, 32), and reorganization of viral membranes (5, 32). Studies with temperature-sensitive (*ts*) and inducible VV mutants have revealed that several proteins interacting with DNA are involved in transition from IV to IMV. Thus, the core protein VP8 (L4R) is thought to be required for correct packaging of the viral genome and/or for the efficient transcription of DNA (61), whereas DNA-binding phosphoprotein VP11 (F18R) (67) and the I7 protein, homologous to yeast type II DNA topoisomerase (24), appear to be essential for

* Corresponding author. Mailing address: Department of Molecular and Cellular Biology, Centro Nacional de Biotecnología, Consejo Superior de Investigaciones Científicas, Campus Universidad Autónoma, Cantoblanco, 28049 Madrid, Spain. Phone: 34-91-585-4503. Fax: 34-91-5854506. E-mail: mesteban@cnb.uam.es.

nucleoid condensation. The A32 protein appears to be required at an earlier step, since repression of A32 results in the accumulation of DNA-deficient IVs (4). Also other DNA-binding proteins, such as the VV early transcription factor VETF, composed of two subunits encoded by the D6R and A8L genes, and the product of the I1L gene are needed for IV-to-IMV transition since viruses deficient in these polypeptides are blocked at the IV stage (19, 20, 27, 29). A similar phenotype is displayed when synthesis of the two structural proteins 39K (A5L) (63) and L1R (38), present in the core and envelope, respectively, is prevented. Proteolytic cleavage of major core proteins P4a (A10L), P4b (A3L), and VP8, which occurs at a late stage of core formation, is apparently required for production of infectious mature virions. Drugs that block virus assembly, such as rifampin and novobiocin, also inhibit the proteolytic processing of these core polypeptides (25, 51). The failure in processing is believed to be an effect secondary to the block in immature envelope formation, which leads to interruption of later stages of viron morphogenesis (25, 68). Repression of the D13L gene, coding for the p65 membrane-associated protein, mimics the effects of rifampin and prevents both viral assembly and protein cleavage (68).

Among the most abundant structural components of the VV is the major core protein P4a, which alone accounts for approximately 14% of the particle's dry weight (49). The 4a polypeptide is a processing product of a higher-molecular-weight precursor P4a (24), which is encoded by the A10L gene (54, 62). P4a is synthesized at late times in the viral infection as a 102-kDa protein, which is posttranslationally cleaved to two smaller polypeptides. The processing occurs at two locations: cleavage at the N-terminal Ala-Gly-Ser site between amino acids 614 and 615 and cleavage at the C-terminal Ala-Gly-Thr site between amino acids 697 and 698 lead to release of 62-kDa (4a) and 23-kDa polypeptides, respectively (55, 56, 59). These cleavage sites are distinct but related to the consensus Ala-Gly-Ala motif for the proteolytic maturation of other VV structural proteins (58). The precursor protein P4a is localized to viral factories and immature virus particles, and both of the cleavage products are associated with the core structure of the mature virion (55, 57). Processing of P4a at these sites should theoretically also yield an intervening 9-kDa polypeptide (amino acids 615 to 697), but its possible localization and fate remain unclear. We have recently described that in the virion, the mature 4a protein forms a complex with the 39K core protein, the product of A5L gene (41), and this interaction may be crucial for the assembly of the core structure.

To investigate the role of the major core protein P4a in VV assembly and life cycle, we have constructed and characterized a conditional virus mutant in which expression of the A10L gene is regulated by the *Escherichia coli lacI* operator-repressor system. By biochemical and electron microscopy analysis, we have defined that this protein is required for correct assembly of the nucleoprotein complex within IVs.

MATERIALS AND METHODS

Cells and viruses. African green monkey kidney (BSC-40) cells and HeLa cells were grown in Dulbecco's modified Eagle's medium (DMEM) supplemented with 10% newborn calf serum. VV strain Western Reserve (WR) was propagated and titrated in BSC-40 cells. Recombinant virus VVindA10L was grown in BSC-40 cells in the presence of 5 mM isopropyl- β -D-thiogalactopyranoside

(IPTG). Viral stocks were partially purified by ultracentrifugation through a 45% sucrose cushion. Further purification of viral particles was performed by banding through 20 to 45% sucrose gradients (15). VVlacI was previously described (42).

Antisera. The rabbit polyclonal anti-P4a (referred to in previous work as anti-62K), 14K, 39K, 15K, and 21K protein sera have been previously described (12, 44, 46), as has the polyclonal serum raised against live VV (45). Rabbit polyclonal antisera against P4b and VP8 were kindly provided by D. Hruby (University of Oregon). A polyclonal serum against the 65K protein was raised by immunization of a rabbit with a synthetic peptide corresponding to amino acids 536 to 550 coupled to keyhole limpet hemocyanin (this peptide was chosen based on the sequence of peptide B1 used by Sodeik et al. [52]). The gold-conjugated goat anti-rabbit serum was purchased from Biocell (Cardiff, United Kingdom).

Plasmid construction. For construction of plasmid transfer vector popA10L-gpt, where the *E. coli lac* operator is inserted immediately downstream of the endogenous A10L gene promoter, two DNA fragments were amplified from VV strain WR (WR VV) genomic DNA by PCR. PCR was performed with primers 1 (5'-**CGGCCGGATGATG-CCTATTAAAGTCATAATAGTAC-3'**) [translation initiation codon for A10L shown in boldface], 2 (5'-**C CGGAATTCTTT ATTGGTGCAATAAACATCC-3'**), 3 (5'-**CGCGGATCCTTTATCTTTA TCATAAACTACTCC-3'**), and 4 (5'-**CGGCCCCGGATTGTATCCGCTCA CAATTATTTATTTAGTATTAAATGACGACCG** [*lac* operator sequence shown in boldface; conserved sequence element TAAAT for transcription initiation of VV late genes {10} shown underlined]). Primers 1 and 2 were used to generate a DNA fragment containing 570 bp of the A10L open reading frame (ORF) (amino acids 1 to 190) flanked by *Eco*RI and *Sma*I restriction sites (restriction sites underlined in primer sequences). Another DNA fragment consisting of VV A11R sequence (amino acids 1 to 152), the entire promoter region between the A10L and A11R ORFs, and *E. coli lac* operator sequence (21 bp), flanked by *Sma*I and *Bam*H I sites, was synthesized using primers 3 and 4. These two PCR-amplified fragments were sequentially cloned into pUC118. The coding sequence for the *E. coli gpt* gene under the VV p7.5 early/late promoter was amplified using primers 5'-TGCAAGCTTAAATAATAAAATACAATAATTAA ATTTCTCG-3' and 5'-ATCAAGCTTTAGCGACCGGAGATTGGCGGGGA C-3', with plasmid pCPURTK13 as a template (17), and ligated into the *Hind*III site of the intermediate plasmid popA10L to create the final VV transfer vector popA10L-gpt. The fidelity of the PCR-amplified gene fragments was confirmed by sequencing. The strategy for construction of the transfer vector popA10L-gpt is illustrated in Fig. 1.

Recombinant virus construction. VVindA10L was isolated by transient dominant selection as previously described (16, 66). All steps of the purification, isolation, and propagation of *lac* repressor-regulated mutant viruses were carried out in the presence of 5 mM IPTG. Briefly, the targeting plasmid popA10L-gpt was transfected into BSC-40 cells infected with VVlacI, which constitutively expresses the *lacI* repressor (42). Selection of the *gpt*-carrying recombinants was performed in the presence of mycophenolic acid (MPA; 25 μ g/ml) and IPTG (5 mM). The intermediate recombinant virus, which contains two copies of the A10L gene, was plaque purified two times in the presence of MPA and IPTG. The following two rounds of purification were performed without MPA selection, which results in the resolution of either VVlacI or VVindA10L where the *gpt* gene is deleted. The *lac* operator-containing plaques were distinguished from the parental virus by PCR screening using oligonucleotide primers 5'-GTCGCA TACTTGTAACTTAG-3' (nucleotides 161 to 141 of A10L) and 5'-ACTACG GCGGCATTATGTTCT-3' (nucleotides 94 to 114 of A11R). The VVindA10L recombinants were subjected to three additional rounds of plaque purification and amplified to produce the virus stocks for subsequent experiments.

VVindA10L growth curves. Confluent monolayers of BSC-40 cells were infected with WR VV or recombinant virus VVindA10L at multiplicities of infection (MOI) of 2.5 and 0.25 PFU/cell. The inoculum was removed after 1 h incubation at 37°C, and the cells were washed twice with DMEM and overlaid with fresh DMEM supplemented with 2% newborn calf serum and containing or lacking IPTG (5 mM). Cells were collected at the indicated times after infection at high or low MOI, and virus yields (PFU per milliliter) were determined by titration on BSC-40 cells in the presence of 5 mM IPTG. To determine the VVlacI input, parallel cultures were maintained at 4°C for the 1-h adsorption period, after which cells were washed twice with DMEM and collected.

Metabolic labeling. BSC-40 cells were infected (5 PFU/cell) with VVlacI or VVindA10L in the presence or absence of 5 mM IPTG. At different times postinfection, cells were washed with methionine-free DMEM and incubated in the same medium for 30 min to deplete intracellular methionine. Cells were then pulse labeled with [35 S]methionine (50 μ Ci/ml) for 30 min, washed three times with ice-cold phosphate-buffered saline (PBS), collected, and lysed in 1× sample buffer (62.5 mM Tris [pH 6.8], 2% sodium dodecyl sulfate [SDS], 0.25% bro-

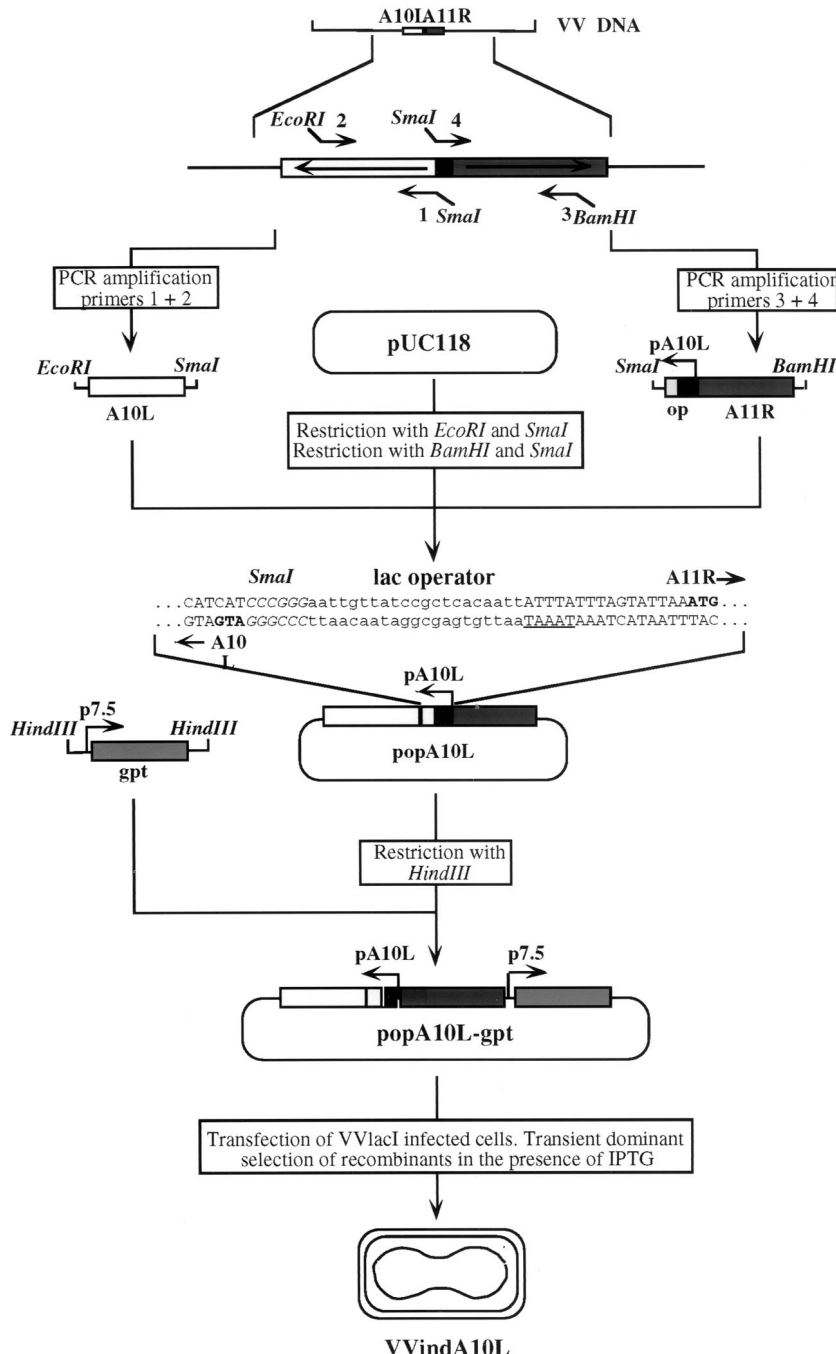


FIG. 1. Construction of the conditional VV recombinant VVindA10L. A DNA fragment corresponding to nucleotides 1 to 570 of the A10L ORF was amplified from VV genomic DNA by PCR using primers 1 and 2 and cloned into pUC118. Another DNA fragment, consisting of a 21-bp *E. coli* *lac* operator (op) sequence, the promoter region between the A10L and A11R genes, and 457 bp of the A11R ORF, was synthesized by PCR amplification using primers 3 and 4 and subsequently cloned into pUC118 carrying the A10L DNA fragment. The sequence around the A10L promoter is shown with A10L and A11R translation initiation codons in boldface, *lac* operator in lowercase, *Sma*I restriction site in italics, and TAAAT consensus sequence for late gene expression underlined. The *E. coli* *gpt* ORF under the control of the VV p7.5 early/late promoter was cloned to the intermediate plasmid popA10L to generate the transfer vector popA10L-gpt. This plasmid was used to transfect BSC-40 cells infected with VVlacI, which constitutively expresses the *E. coli* *lac* repressor. Transient dominant selection was used to isolate the VVindA10L recombinants in the presence of 5 mM IPTG. Sequences of the primers used are given in Materials and Methods.

mophenol blue, 5% glycerol, 5% 2-mercaptoethanol). Samples were boiled for 5 min, and proteins were fractionated by SDS-polyacrylamide gel electrophoresis (SDS-PAGE) and transferred to a nitrocellulose membrane. Labeled proteins were visualized after autoradiography.

Western blot analysis. Viral proteins from purified virions or extracts from virus-infected cells were fractionated by SDS-PAGE, transferred to nitrocellulose, and incubated with different antibodies specific to VV proteins. After incubation with a peroxidase-conjugated secondary antibody, immunoreactive

bands were detected either by color development after incubation with chloronaphthol as described elsewhere (42) or by chemiluminescence (ECL kit; Amersham).

DNA analysis of purified virions. Viral particles from WR VV and VVindA10L were purified by centrifugation through a 45% sucrose cushion and banding on 20 to 45% sucrose gradient. Purified virions were pelleted and resuspended in 1 mM Na₂HPO₄ buffer, and the number of particles was determined by measuring the optical density of virus preparations (1 unit of optical density at 260 nm is equivalent to 1.2×10^{10} particles/ml [23]). The protein content in these samples was determined by the Bradford assay using a bicinchoninic acid kit (Pierce). Viral suspensions containing approximately the same amount of viral particles were prepared in PBS. Twofold dilutions made from these starting virus suspensions were applied in duplicate to nitrocellulose membranes in a vacuum manifold. One of the membranes was incubated with anti-VV antibodies in 5% BLOTO followed by incubation with peroxidase-conjugated goat anti-rabbit immunoglobulin G. Antibody reactivity was detected by chemiluminescence. The twin membrane was blotted on paper filter saturated with 0.5 M NaOH, then on paper saturated with 1 M Tris-HCl (pH 7.5)-1.5 M NaCl, and finally on paper saturated with 2× SSC (1× SSC is 0.15 M NaCl plus 0.015 M sodium citrate). The viral DNA was UV cross-linked to the membrane and hybridized with a probe prepared by ³²P labeling of purified VV DNA. Hybridization was carried out by standard procedures. The radioactive DNA signal was visualized by autoradiography.

Electron microscopy. (i) **Negative staining of purified virions.** Suspensions of purified WR VV and VVindA10L IMVs were treated as described elsewhere (44). Virions were adsorbed to electron microscopy grids coated with collodion and carbon and made hydrophilic by glow discharge. After washing in distilled water, samples were stained with a 2% solution of uranyl acetate for 30 s, allowed to dry, and studied by electron microscopy.

(ii) **Embedding of infected cells and isolated virions in EML-812.** Monolayers of HeLa cells were infected at an MOI of 5 PFU/cell with WR VV or VVindA10L in the presence or absence of IPTG. At 24 h postinfection (hpi), cells were fixed *in situ* with a mixture of 2% glutaraldehyde and 1% tannic acid in 0.4 M HEPES buffer (pH 7.5) for 1 h at room temperature. Suspensions of purified WR VV or VVindA10L virions were fixed with the same mixture under identical conditions. Fixed monolayers were removed from the culture dishes in the fixative and transferred to Eppendorf tubes. After centrifugation and washing with HEPES buffer, the cells or the virions were processed for embedding in the resin TAAB 812 (TAAB Laboratories Ltd., Berkshire, United Kingdom) as previously described (39, 40, 47). Ultrathin (around 30-nm) sections of the samples were obtained and stained with saturated uranyl acetate and lead citrate by standard procedures.

(iii) **Embedding of infected cells in Lowicryl K4M for immunogold labeling.** Infected cells were submitted to a mild fixation *in situ* with a mixture of 4% paraformaldehyde and 0.1% glutaraldehyde in PBS (pH 7.4) for 30 min at 4°C. Cells were removed from the culture dishes in the fixative, centrifuged, and washed with PBS to be processed for embedding in Lowicryl K4M at room temperature as previously described (39, 46, 48). Ultrathin sections were collected on gold grids coated with Formvar and carbon and processed for immunogold detection of VV proteins as previously described in detail (46).

(iv) **Detection of DNA on ultrathin sections.** For DNA detection, freshly obtained sections of infected cells embedded in Lowicryl K4M were used. Sections were treated for conventional immunogold labeling using a monoclonal antibody specific for single-stranded and double-stranded DNA (Chemicon International, Inc., Temecula, Calif.) diluted 1:300 in Tris buffer-gelatin (30 mM Tris-HCl [pH 8.0] containing 150 mM NaCl, 0.1% bovine serum albumin, and 1% gelatin) and a gold conjugate of goat anti-mouse and 10-nm colloidal gold particles according to standard immunogold procedures (39, 48). DNA on the surface of the sections was also detected as described by Bendayan (1), using a conjugate of DNase I and colloidal gold particles of 10 nm (E-Y Laboratories, Inc., San Mateo, Calif.). Sections were preincubated for 15 min with PBS (pH 6.0) containing 0.02 mg of polyethylene glycol 8000 (PEG) per ml (PBS-PEG, pH 6.0) for 1 h and washed with PBS-PEG (six times for 5 min each). After fixation with glutaraldehyde (2.5% in PBS-PEG) for 10 min and washing with distilled water (five times for 2 min each), sections were stained with saturated uranyl acetate for 25 min, washed with water, and dried. Some sections were pretreated with nonconjugated DNase I (1 mg/ml) 1 h at 37°C, washed with water, and dried before incubation with PBS-PEG and DNase-gold. Samples were studied in a JEOL 1200 EX II electron microscope.

RESULTS

Construction of a recombinant VV with an inducible A10L gene. P4a, the product of the A10L ORF, is the major structural core polypeptide of VV (49). Its proteolytic processing is believed to be essential for the production of infectious mature virus particles. However, the possible functions of the precursor form P4a or its cleavage products 4a (62 kDa) and 23-kDa proteins have not been studied. To investigate the role(s) of these polypeptides in the virus life cycle and morphogenesis, we constructed and characterized an inducible VV recombinant, VVindA10L, in which the synthesis of P4a is under the control of the *E. coli lacI* operator-repressor system. The standard method where by the *lac* operator sequence is placed adjacent to the promoter of the target gene (66, 68) was used in this work. Briefly, VVindA10L was generated starting with recombinant virus VVlacI, containing in the nonessential thymidine kinase locus of VV genome the *lacI* repressor gene driven by the VV constitutive p7.5 promoter (42). Plasmid popA10L-gpt, containing (i) the *lac* operator between the endogenous promoter and the initiation codon ATG for A10L and (ii) the p7.5-regulated *E. coli gpt* gene for transient dominant selection of the viral recombinants (16, 61), was generated by recombinant PCR and transfected to VVlacI-infected cells. The strategy followed to construct the operator-controlled A10L gene is depicted in Fig. 1. Two successful homologous recombination events resulted in the replacement of endogenous A10L gene with the mutated copy and deletion of the *gpt* marker gene. DNA samples from 43 individual plaque isolates were screened by PCR for the presence of the *lac* operator, using primers flanking the site of insertion. The sizes of the PCR products for the wild-type (WT) and *lac* operator-mutated forms of the A10L gene were 289 and 310 bp, respectively (data not shown). Nine (21%) of the 43 samples analyzed were found to contain the 21-bp operator sequence, 12 (28%) corresponded to the parental virus, and 22 (51%) contained both forms of the PCR product. These were interpreted to represent single-crossover recombination intermediates where two copies of the A10L gene are arranged in tandem. Several of the operator-containing inducible mutants were plaque purified two or three additional times, and virus from these plaques was amplified in the presence of 5 mM IPTG to produce virus stocks. As determined by PCR, the mutant A10L viruses were found free of parental VVlacI virus.

IPTG-dependent expression of the A10L gene. To ensure that A10L gene expression was regulated by IPTG, BSC-40 cells were infected with the mutant virus VVindA10L or with the parental virus VVlacI in the absence or presence of IPTG. At 24 hpi, cells were collected and cell extracts were analyzed by Western blotting with anti-P4a antibodies. As shown in Fig. 2A, the P4a precursor and its cleavage product 4a were clearly observed in extracts from cells infected with VVindA10L in the presence of IPTG (lane 3), although the level of A10L gene expression was lower than in cells infected with WR VV (lanes 1 and 2) or VVlacI (lanes 5 and 6) with or without IPTG, and cleavage of the P4a precursor was also diminished. On the other hand, in cells infected with VVindA10L in the absence of IPTG, P4a and 4a proteins can be barely detected (lane 4). The minimal expression of these proteins under these conditions may be due to the presence in the virus stock of a minor

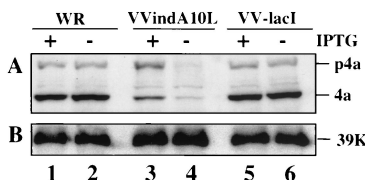


FIG. 2. Inducible expression of P4a in VVindA10L-infected cells. BSC-40 cells were infected (5 PFU/cell) with WR (lanes 1 and 2), VVindA10L (lanes 3 and 4), or VVlacI (lanes 5 and 6) in the presence or absence of IPTG, as indicated at the top. At 24 hpi, cells were harvested, and proteins were separated by SDS-PAGE (10% polyacrylamide gel) and transferred to a nitrocellulose membrane. The membrane was excised in two parts; the upper one was reacted with anti-P4a/4a antibodies (A), and the lower one was incubated with anti-39K antibodies (B). Protein bands were developed by chemiluminescence after incubation with a secondary peroxidase-conjugated goat anti-rabbit serum. Positions of the P4a, 4a, and 39K proteins are indicated at the right side.

amount of mutant viruses that escape *lac* operator repression (discussed below).

When the same blot was developed with an antibody to the VV 39K protein, similar amounts of this protein were detected in extracts from cells infected with VVindA10L, WR, or VVlacI (Fig. 2B), indicating that the observed differences in A10L gene expression were not due to an overall reduction in viral protein synthesis.

Replication of VVindA10L under permissive and nonpermissive conditions. To determine the possible effect of A10L gene repression on virus replication and cell-to-cell spread, we compared plaque formation by VVindA10L in the presence and absence of the inducer IPTG with that by the parental virus VVlacI. Figure 3A shows that omission of IPTG after infection with VVindA10L resulted in a marked reduction, of about 95%, in the number of plaques with respect to the values obtained when infections were carried out under permissive (with IPTG) conditions. Moreover, while plaques made by VVindA10L in the presence of the inducer were all slightly smaller than those produced by the parental virus, in cells infected by the mutant in the absence of IPTG, small and large plaques were formed. Large plaques are probably due to some repressor escape mutants that arise during VVindA10L infection under restrictive conditions, as has been indicated for other VV-inducible mutants (43, 47, 61, 68). In addition, we have determined viral yields after infection at both high (2.5 PFU/cell) and low (0.25 PFU/cell) MOI. Titration of virus from cells infected for 24 h with 2.5 PFU of VVindA10L per cell in the absence of IPTG showed a reduction of virus yields of about 2 log units compared to VVlacI-infected cells (Fig. 3B). In the presence of the inducer, virus yields were only partially recovered. Under these conditions, the maximum titer was reached at 24 hpi, and it was more than 1 log lower than VVlacI titers. This result is in accordance with the smaller plaque size phenotype displayed by the mutant. In addition, when infection of cell cultures was performed at a low MOI, the yield obtained by 24 hpi in the presence of the inducer was more than 2 log units higher than the yield attained when IPTG was omitted (Fig. 3C). Moreover, the progeny virus grown under these nonpermissive conditions was shown to escape regulation by IPTG, since the same titers were obtained when titrations were performed in the presence or absence of

the inducer (not shown). Again, this result indicates that in the VVindA10L stock there is a minor population of virus that escape *lacI* repression. From the growth characteristics of VVindA10L, we can conclude that the A10L gene product is essential during the virus life cycle.

Viral protein synthesis in cells infected with VVindA10L. To examine whether repression of the A10L gene has any effect on the pattern and/or the timing of viral protein synthesis, cells infected with VVindA10L in the absence or presence of the inducer were pulse-labeled with [³⁵S]methionine for 30 min at different times postinfection. As shown in Fig. 4A, both in the absence and in the presence of IPTG, there was a delay in the appearance of viral proteins and the concomitant shutoff of host protein synthesis compared with extracts of cells infected with the control virus VVlacI. While in VVlacI-infected cells late proteins were clearly visible by 6 hpi (lane 8), it took 8 h to first visualize some of these proteins in cells infected with the mutant virus (lanes 12 and 13), and the increase in the amount of these proteins was most obvious at 24 hpi. Thus, despite the initial delay, by 24 hpi the rate of protein synthesis appeared to be similar in VVlacI- and mutant-infected cells (compare lanes 14 to 16). The profile of proteins synthesized in VVindA10L-infected cells in the presence or absence of the inducer were almost indistinguishable except for the absence in the latter case of a band corresponding in size to P4a and the reduced amount of a protein that was later identified by Western blotting as the 4b cleavage product (see below). These two products were also reduced in amount in proteins synthesized in cells infected by VVindA10L under permissive conditions compared with VVlacI-infected cells (compare lanes 14 and 15). In cells infected with the mutant, with or without IPTG, there were three additional bands which were not detected in VVlacI-infected cells.

To identify some of the radioactive proteins after separation by SDS-PAGE, proteins were transferred to nitrocellulose and probed in Western blot analysis with different antibodies to VV proteins P4a, P4b, VP8, 39K, and p65 (D13L). Surprisingly, while in cells infected with VVlacI most proteins could be first detected by 6 hpi (Fig. 4B, lane 8), in VVindA10L-infected cells all proteins assayed were present at any time postinfection, even at the earliest time point tested (2 hpi) (lanes 3 and 4), and the amount of each of these proteins did not increase over the time until 8 or 24 hpi, when there was a clear enhancement in the intensity of the corresponding protein bands. Since the proteins analyzed are all components of the viral particle, their presence from the beginning of the infection indicates that a large amount of the input virus remained associated with the cells. With the anti-P4a antibodies (blot a), we confirmed that by 24 hpi only a minor amount of this protein was accumulated in cells infected with the mutant without IPTG (lane 16), but the protein was readily synthesized when IPTG was added (lane 15), although both the total amount of protein and the rate of proteolytic processing of the P4a precursor were reduced compared with cells infected with the parental virus (lane 14). The bands corresponding to P4b and 4b products were also identified after reactivity with the specific antibody (blot b). In the autoradiogram, the 4b cleavage product was not discernible among the proteins synthesized at 24 hpi in cells infected with the mutant in the absence of IPTG (Fig. 4A, lane 16), and a reduced amount of this

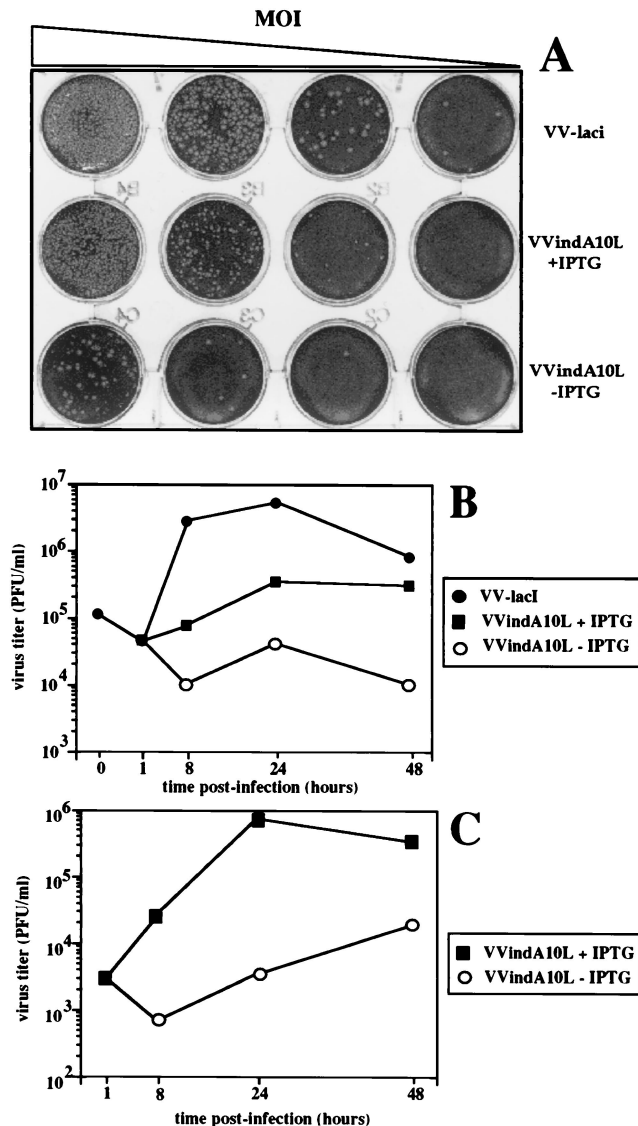


FIG. 3. VVindA10L virus growth is dependent on the presence of IPTG. (A) Plaque assay. Confluent monolayers of BSC-40 cells were infected with 10-fold dilutions of either VVlacI or VVindA10L stocks and overlaid with DMEM supplemented with 2% newborn calf serum and containing or lacking 5 mM IPTG. After 2 days, the monolayers were stained with 1% crystal violet. (B) One-step growth curves. BSC-40 cells were infected at an MOI of 2.5 PFU/cell with VVlacI or VVindA10L in the presence or absence of 5 mM IPTG. (C) Multiple-step growth curves. BSC-40 cells were infected at an MOI of 0.25 PFU/cell with VVindA10L in the presence or absence of 5 mM IPTG. Cells infected at high or low MOI were harvested just after the adsorption (1-h time point) or at various times postinfection (8, 24, and 48, hpi), and progeny viruses were titrated by plaque assay on monolayers of BSC-40 cells in the presence of IPTG. The titer of VVlacI at time zero corresponds to the virus remaining after a 1-h adsorption period at 4°C.

product was observed when infection was performed in the presence of IPTG (lane 15) compared with the amount detected in extracts from VVlacI-infected cells (lane 14). This result suggests that proteolytic processing of P4b was very inefficient in cells infected by the mutant without IPTG (lane 16) and still poorly efficient in the presence of the inducer.

Similarly, cleavage of VP8 precursor was somewhat inhibited in cells infected with the mutant plus IPTG, and less processing was observed in the absence of IPTG (compare lanes 14 to 16 in Fig. 4B, blot c).

The 39K and 65K proteins were also present in VVindA10L-infected cells from the first time point postinfection tested, and the amount of these two products began to increase by 6 to 8 hpi (blots d and e).

Thus, from this experiment we conclude that A10L gene expression is not essential for viral protein synthesis but is required for proteolytic processing of the two other major core proteins, P4b and VP8.

VV morphogenesis is interrupted when synthesis of the A10L gene is repressed. The lethal phenotype displayed by VVindA10L under nonpermissive conditions and the inefficient proteolytic processing of the major core precursors are both indicative of a blockade in virion morphogenesis. Thus, we examined by electron microscopy thin sections of cells infected with VVindA10L in the presence and absence of IPTG.

Empty, spherical IV-like virions, as well as aberrant IV particles with very dense internal material, accumulate in the cytoplasm of HeLa cells infected with the VVindA10L recombinant virus. Neither normal IVs nor IMVs were detected, and large dense aggregates that organize in bands accumulated in the cytoplasm of these cells (Figs. 5B, 6A, and 6B). Similar, though smaller, aggregates are also occasionally seen in HeLa cells infected with WR VV at long postinfection times (not shown). In the presence of IPTG, characteristic IVs coexist with empty or abnormal IV-like particles. In this case, IMV-like virions were able to form, although most of them were round (Fig. 5D and 6). Interestingly, dense material entering IVs is also frequently seen (Figs. 5C and 6B). These results strongly suggest that the organization of the IV content is clearly disturbed in this mutant, while the process of envelope formation is indistinguishable from that observed in WR VV-infected cells. Immunogold detection of VV proteins also points to this fact. While the envelope proteins 21K (A17L), 15K (A14L), and 65K localized in the viral crescents or in the envelope of IV-like particles (Fig. 7), the core protein VP8 was almost absent, as indicated by immunogold labeling on sections (Fig. 8). Signal associated with the 39K protein was variable in IV-like particles. Scattered labeling around viral particles was also detected (Fig. 8A and 8B). Although differences between the samples with IPTG and without IPTG were not dramatic, labeling in the latter was more heterogeneous, with a higher percentage of IV-like particles exhibiting no signal. Regarding the 14K (A27L) envelope protein, it has been previously shown that in the absence of virion assembly the protein is dispersed throughout the cytoplasm (44), and in normal infections this protein can be first seen associated with viral membranes at a transition stage of virion assembly between IV and IMV (53). Thus, it is not surprising the scattered distribution of this protein in the cytoplasm of VVindA10L infected cells where it also localizes in cytoplasmic aggregated material (Fig. 7D).

The strong electron density of the large aggregates seen in the cytoplasm of VVindA10L-infected cells, together with the fact that they appear in most cases in contact with or even inside IVs (Fig. 5 and 6B), indicates that they may represent nucleoprotein complexes. To analyze this possibility, we used

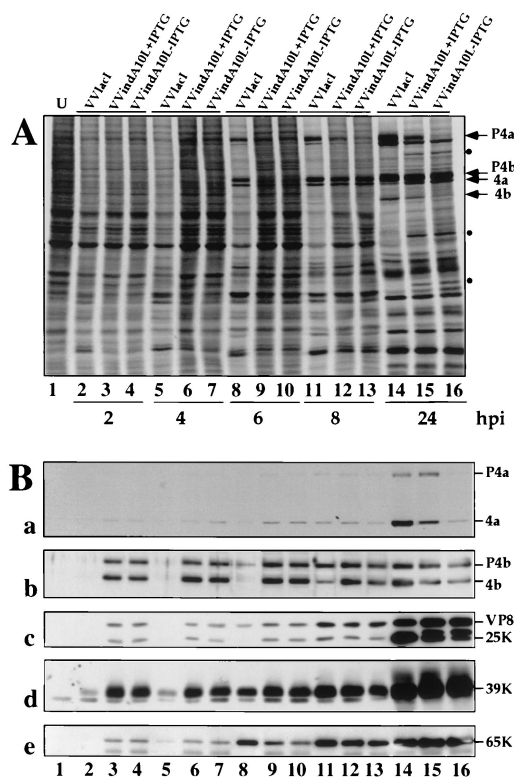


FIG. 4. Synthesis of viral proteins. BSC-40 cells were infected (5 PFU/cell) with VVlacI or VVindA10L in the presence or absence of 5 mM IPTG. At different times postinfection (indicated below panel A), cells were pulse-labeled with [³⁵S]methionine (50 μ Ci/ml) for 30 min. A lysate from ³⁵S-labeled uninfected cells (U) was included as a control. Proteins were fractionated by SDS-PAGE (10% polyacrylamide gel) and transferred to a nitrocellulose membrane. (A) ³⁵S-labeled proteins were visualized after autoradiography of the nitrocellulose membrane. (B) Western blot analysis of the transferred proteins with antibodies against the P4a, P4b, VP8, 39K, and 65K proteins.

either anti-DNA antibodies followed by gold-conjugated anti-immunoglobulin G or directly gold-conjugated DNase. DNA localization on thin sections of infected cells provided clear signals in cellular chromatin and the interior of IMVs, as well as in the large, dense aggregates accumulated in the cytoplasm and the interior of some IV-like particles (Fig. 9A to D). The specificity of the signal is indicated by the fact that when sections were preincubated with nonconjugated DNase for 1 h at 37°C before the addition of the anti-DNA antibodies or the DNase-gold labeling was precluded (Fig. 9E).

However, immunogold localization of VV proteins was not affected by DNase treatment (not shown). Among the various antibodies against VV core or membrane proteins tested, only the anti-39K antibody provided weak but repetitive signals in

these dense structures (Fig. 8A). These results indicate that viral DNA organization and packaging seem to be significantly impaired in the absence of P4a.

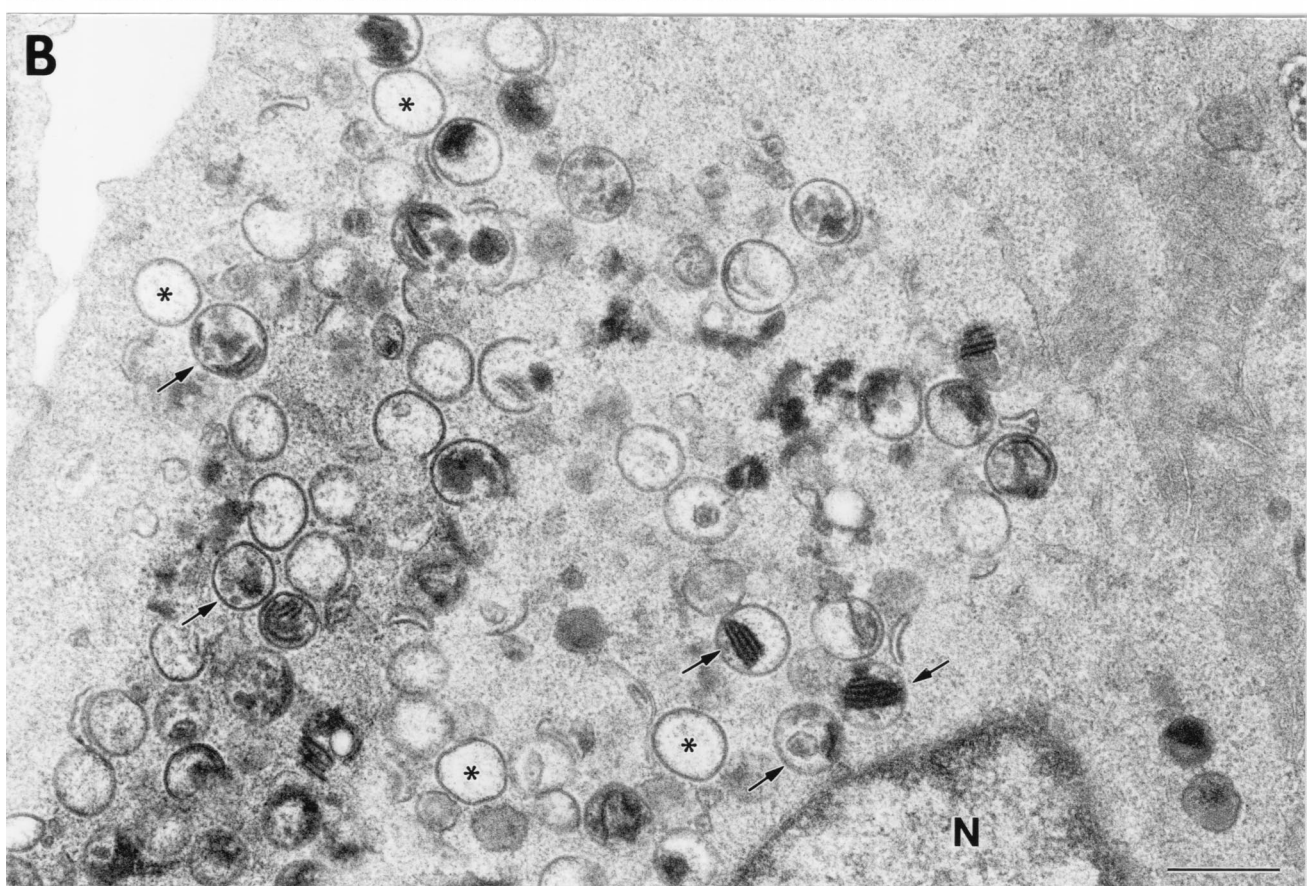
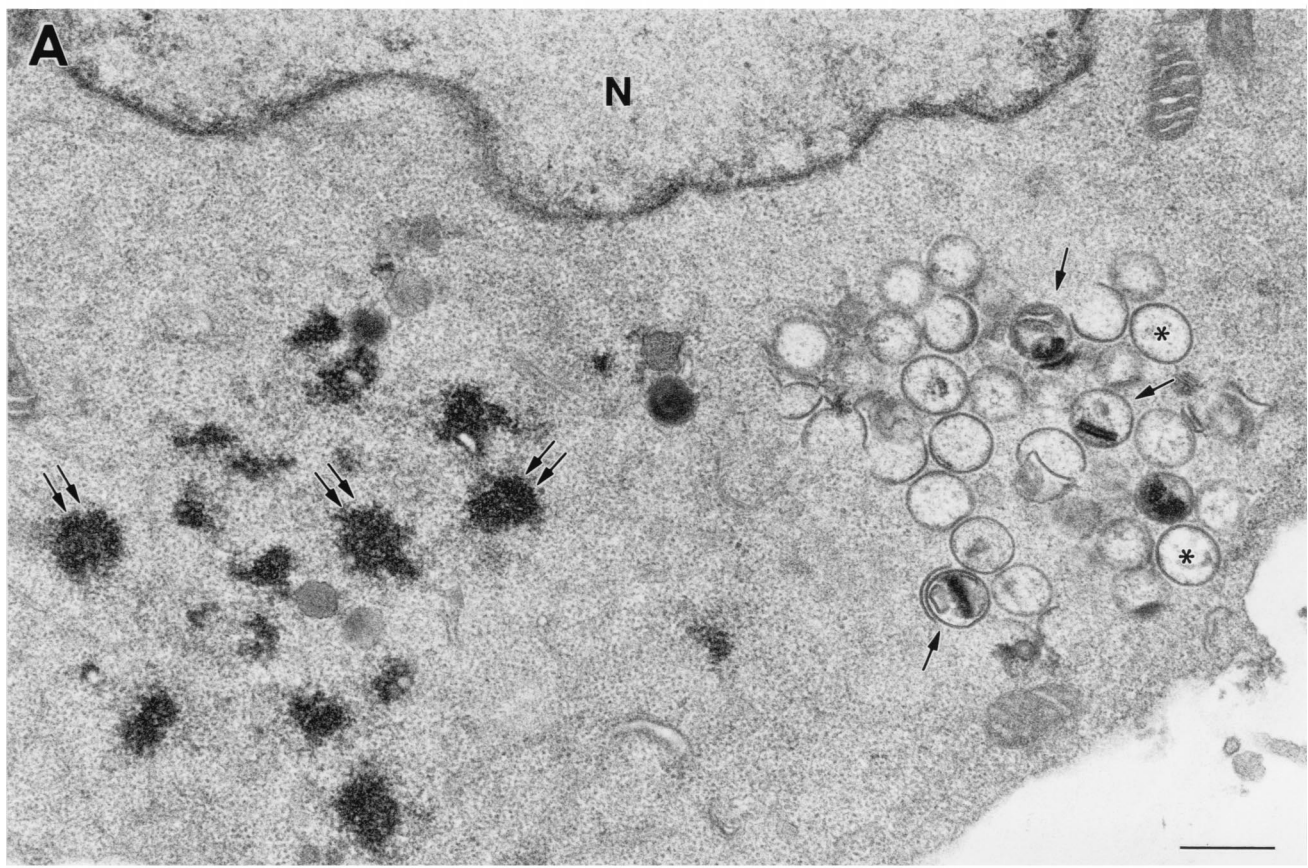
Characteristics of viral particles purified from cells infected with VVindA10L under permissive conditions. We have observed that even in the presence of the inducer VVindA10L, growth is compromised and low yields of progeny virus are obtained. Moreover, electron microscopy examination of cells infected under these conditions showed the presence of a high amount of abnormally rounded IMV-like particles. The fact that at late times after infection with VVindA10L under permissive or nonpermissive conditions we still could detect core and membrane proteins from the input virus, and in large quantity, suggests that these IMV-like particles may not be infectious but may remain attached to the cell membrane. Thus, we examined the characteristics of particles purified from cells infected with VVindA10L in the presence of IPTG in comparison with those produced after infection with WR VV and purified in parallel by banding on sucrose gradients. Similarly cloudy bands were obtained from both VVindA10L and WR preparations, although the protein concentration in the WR sample was about double than that in VVindA10L, indicating that the former contains twice the amount of particles as the latter. Next, we determined the infectivity of these preparations by plaque assay in the presence of the inducer. As the previous result had suggested, the infectivity of VVindA10L particles was reduced to about 10% with respect to WR. This 10% infectivity correlates well with the estimated frequency of appearance of normal brick-shaped IMVs in cells infected by VVindA10L plus IPTG, as determined by electron microscopy of thin sections from infected cells.

(i) **Ultrastructural analysis.** The preparations of purified virions were also examined by electron microscopy in two ways by negative staining and in ultrathin section. By negative staining, most VVindA10L particles were spherical (Fig. 10B), and again, only about 10% showed the characteristic brick shape of VV. In ultrathin sections, VVindA10L particles appeared irregularly shaped, although a core-like structure could be distinguished in the interior (Fig. 10D). By contrast, the majority (90%) of WR particles purified and handled in parallel showed a typical brick-shaped or ovoid appearance, both by negative staining (Fig. 10A) and in ultrathin sections (Fig. 10C).

(ii) **Biochemical analysis.** In an attempt to understand the basis for the low infectivity of the viral particles produced by VVindA10L plus IPTG, we analyzed both their DNA content and protein composition. To determine whether these deficient IMV-like particles had incorporated the genomic DNA, we performed a slot-blot DNA hybridization assay. For this, twofold dilutions of the purified virus preparations from VVindA10L and WR were applied in parallel to nitrocellulose. Two replicas were generated; one was hybridized with a ³²P-

FIG. 5. Low-magnification fields of HeLa cells infected for 24 h with VVindA10L in the absence (A and B) or presence (C and D) of IPTG. The cytoplasm of cells infected with VVindA10L in the absence of IPTG shows areas that exclude cellular organelles with electron-dense spots (double arrows in panel A) and spherical IV-like structures. Some of these are similar to IVs but apparently devoid of electron-dense viroplasmic material (asterisks), while some others are clearly different and contain very dense material or membranous structures (arrows). When HeLa cells are infected with VVindA10L in the presence of IPTG, characteristic IVs together with IV-like particles are seen (asterisks mark empty IVs, while arrows point to IVs containing membranes or very dense material). Cytoplasmic very dense filamentous structures (arrowheads) and round IMV-like particles (marked IMV*) can be also distinguished. N, nucleus; bars, 0.5 μ m.

VVindA10L - IPTG



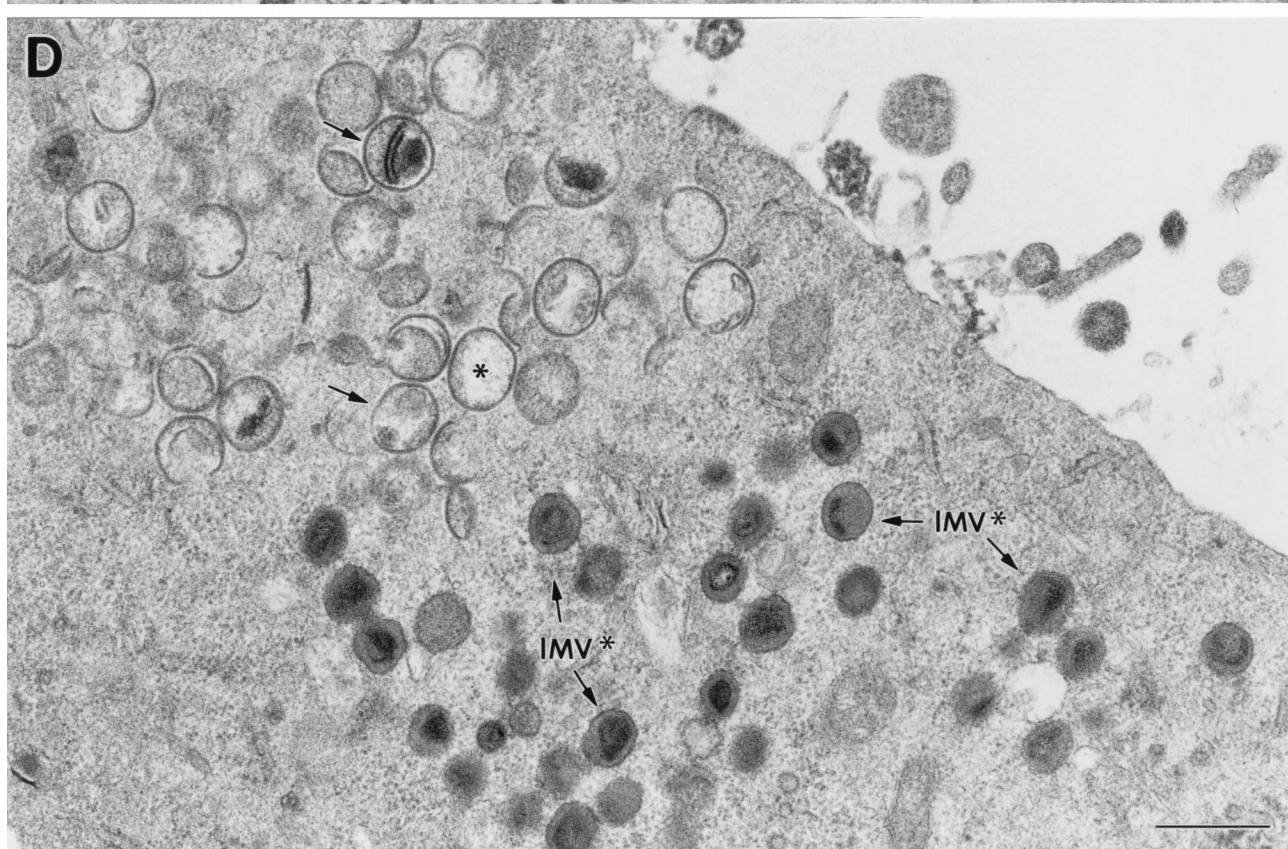
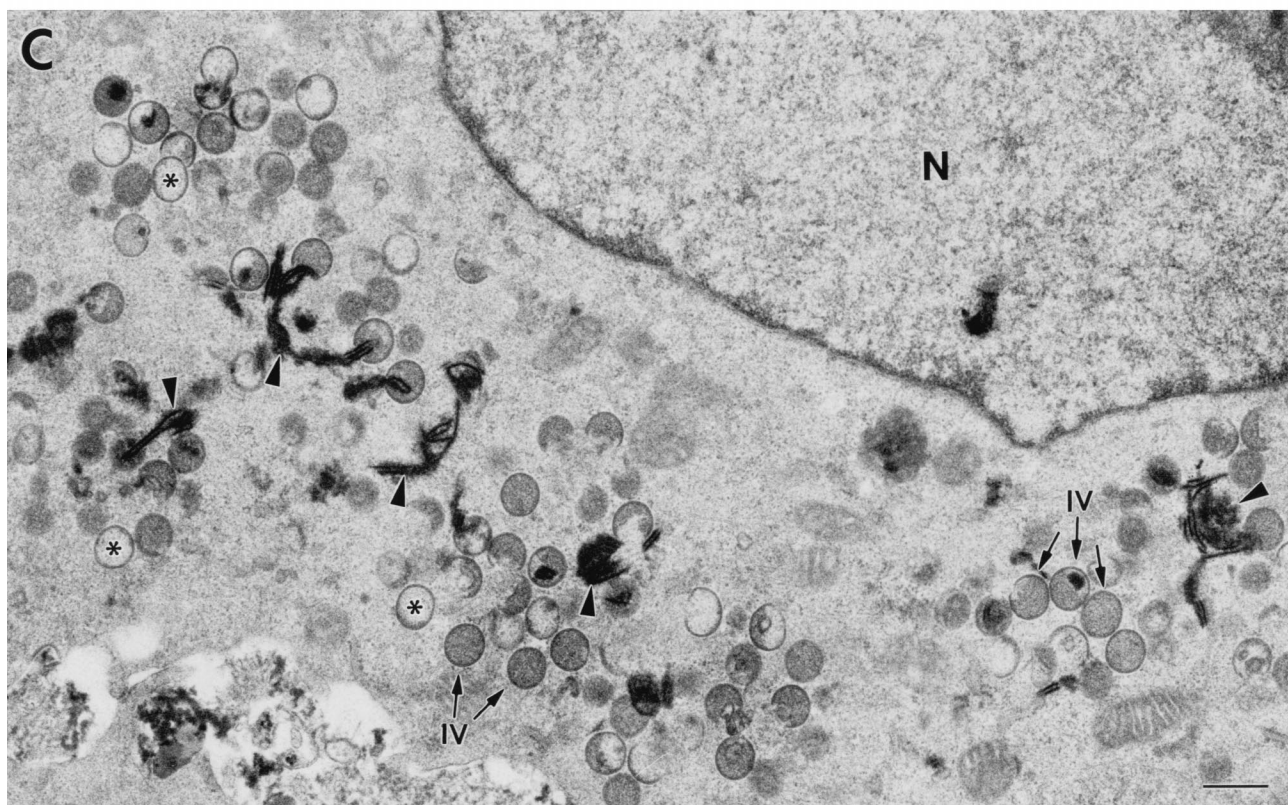
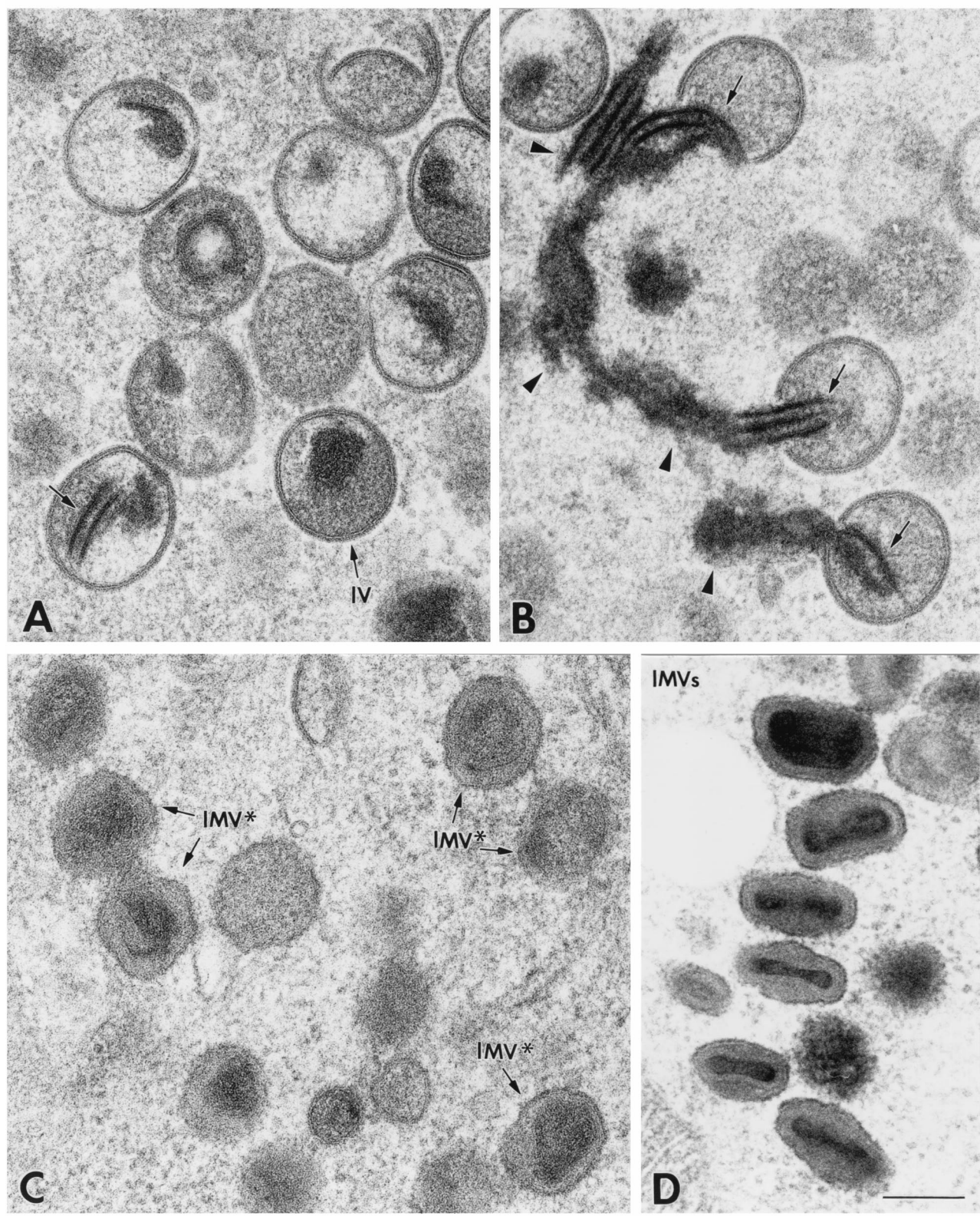
VVindA10L + IPTG

FIG. 5—Continued.

VVindA10L + IPTG



WRVV

FIG. 6. High-magnification fields of different types of viral particles formed in HeLa cells infected for 24 h with VVindA10L in the presence of IPTG (A to C) or with WR VV (D). (A and B) Characteristic IVs are seen near numerous IV-like particles of abnormal content. Very electron-dense material (arrowheads) that organizes in regularly spaced bands accumulates in the cytoplasm and can also be seen inside IV-like particles (arrows). (C) IMV-like particles (marked IMV*) formed in these cells contain a dense core and have an abnormal round shape compared with WR VV IMVs (D). Bar, 200 nm.

VVindA10L - IPTG

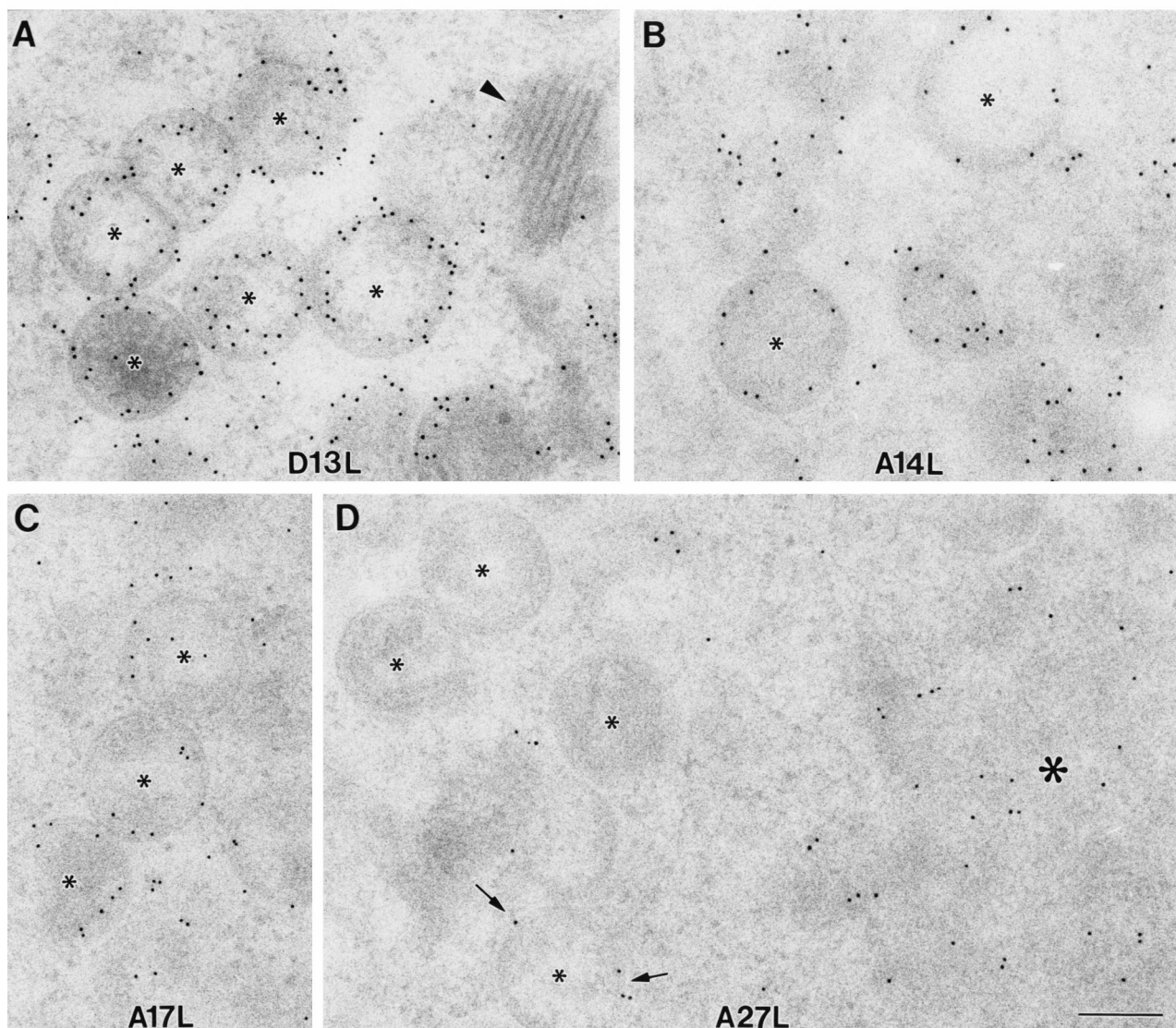


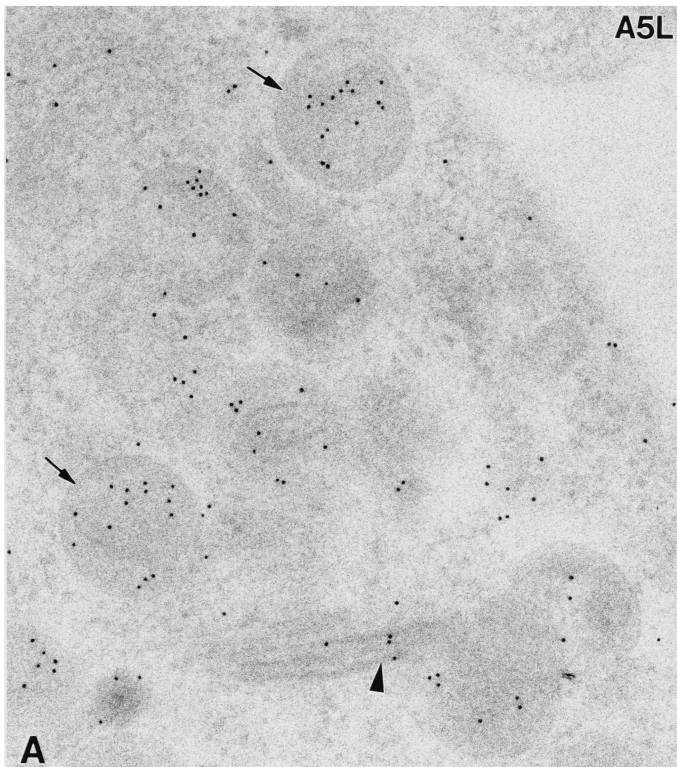
FIG. 7. Immunogold labeling of VV envelope proteins in HeLa cells infected with VVindA10L in the absence of IPTG. Rabbit polyclonal antisera and a conjugate of secondary antibody and colloidal gold (10 nm) were used (see Materials and Methods) to localize 65K (A), 15K (B), 21K (C), and 14K (D) proteins, the products of genes D13L, A14L, A17L, and A27L, respectively. (A to C) In all cases, labeling is mainly concentrated in the curved crescents of IV-like particles (small asterisks), with no labeling associated to the very dense material of regular bands (arrowhead). (D) The 14K protein seems to form cytoplasmic accumulations (large asterisk), and only a few IV-like particles present a weak peripheral signal (arrows). Bar, 200 nm.

probe specific for VV viral DNA, while the other was reacted with an anti-VV polyclonal serum as a control for the amount of virus loaded. As shown in Fig. 11, there were no differences in the amount of DNA between VVindA10L and WR parti-

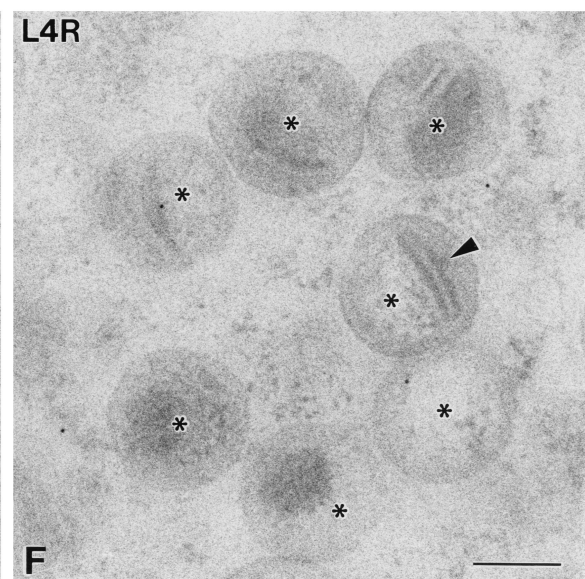
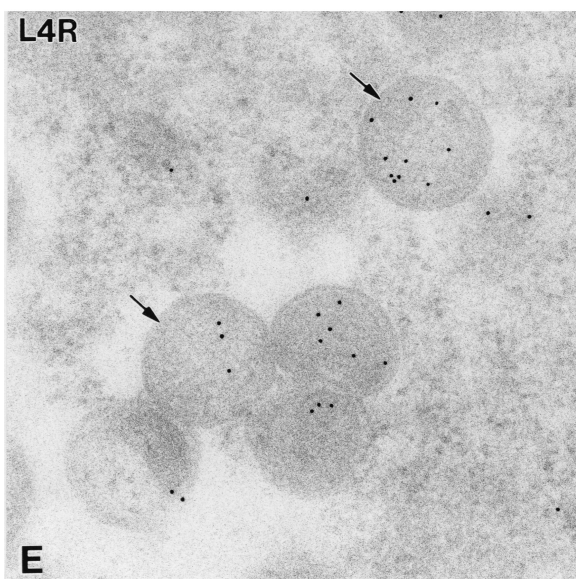
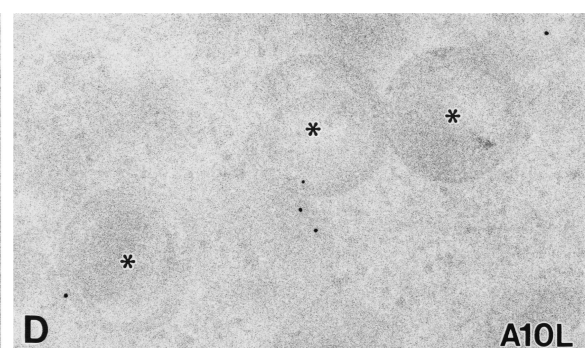
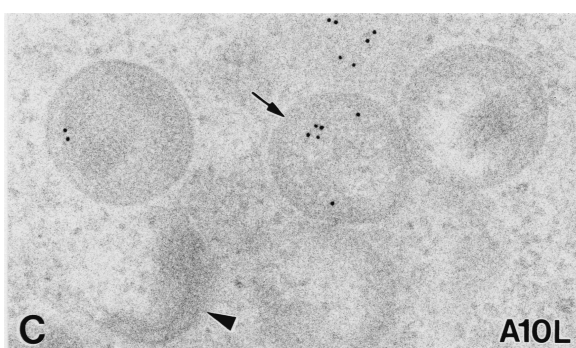
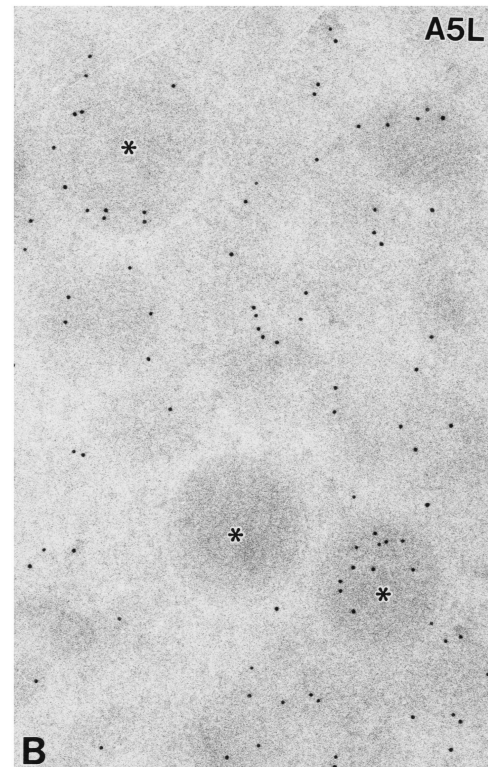
cles. Next, the protein composition of VVindA10L particles was analyzed by Western blotting in comparison to WR particles. The patterns of proteins detected by a polyclonal anti-VV serum were very similar for both preparations, although in

FIG. 8. Immunogold detection of VV core proteins in HeLa cells infected with VVindA10L in the presence (A, C, and E) or absence (B, D, and F) of IPTG. Rabbit polyclonal antisera and a conjugate of secondary antibody and colloidal gold (10 nm) were used to localized 39K (A and B), P4a (C and D), and VP8 (E and F), the products of genes A4L, A10L, and L4R, respectively. (A) Labeling associated with 39K is seen scattered in the cytoplasm and inside IVs (arrows). A weak labeling associated to the very dense cytoplasmic bands is also usually seen (arrowhead). (B) IV-like particles formed in the absence of IPTG (asterisks) contain a variable amount and distribution pattern of gold particles. Labeling associated with P4a is weak in the viral particles formed in the presence of IPTG (arrow in panel C) and absent both in the very dense cytoplasmic bands (arrowhead in C) and in IV-like particles formed in the absence of IPTG (asterisks in panel D). The VP8 nucleoprotein localizes inside IVs assembled in the presence of IPTG (arrows in panel E), while IV-like particles formed in the absence of the inducer (asterisks in panel F) are almost totally devoid of signal. Bar, 200 nm.

VVindA10L + IPTG



VVindA10L - IPTG



VVindA10L there was an additional high-molecular-weight protein, corresponding in size to the uncleaved P4a (not shown). The presence of P4a precursor in VVindA10L purified virions was confirmed after reactivity of the fractionated virion proteins with specific anti-P4a/4a antibodies (Fig. 12, lane 4). A remnant of P4b precursor was also detected in purified particles from VVindA10L (lane 2). Neither P4a nor P4b was detected in the WR preparation (lanes 1 and 3). This result indicates that the abnormal particles observed in this preparation may represent intermediate forms in the IV-to-IMV maturation process.

DISCUSSION

VV particles are complex macromolecular structures that contain about 100 different polypeptides, including, in addition to structural proteins, the complete machinery for early gene expression (19, 20, 69). Important and still unresolved issues about VV assembly are how the full complement of proteins become wrapped by the viral membrane to generate individual spherical IVs and how the genomic DNA is incorporated into these particles. Several studies suggested that the viral DNA packed into a nucleoprotein complex is taken up before the IVs are completely sealed (13, 18, 28, 31).

Structural proteins localized in the internal core of the mature IMVs are major components of the viroplasmic matrix of the viral factories and IVs (57). Thus, it is reasonable to assume that inhibition of synthesis of any of these proteins will have a major impact on VV assembly. In the present report, we describe the generation of a conditional mutant that inducibly expresses the A10L gene coding for one of the most abundant protein of the virion, P4a. For this purpose we modified the endogenous A10L gene by introducing the *lac* operator sequence between the A10L promoter and the initiation codon in the context of a recombinant VV that constitutively expresses the *lacI* repressor (VV*lacI*) (42). Mutant viruses (VVindA10L) were selected by the transient dominant selection method (16, 66). By Western blot analysis, we demonstrated that in cells infected with VVindA10L, the expression of the P4a precursor and the 4a cleaved product is dependent on the presence of IPTG in the culture medium. However, even under these permissive conditions both expression and proteolytic cleavage of P4a are clearly reduced compared with cells infected with the parental virus VV*lacI*. This is interpreted as the result of incomplete derepression, since the amount of the 39K core protein used as the control differed little in both VVindA10L- and VV*lacI*-infected cultures with or without IPTG.

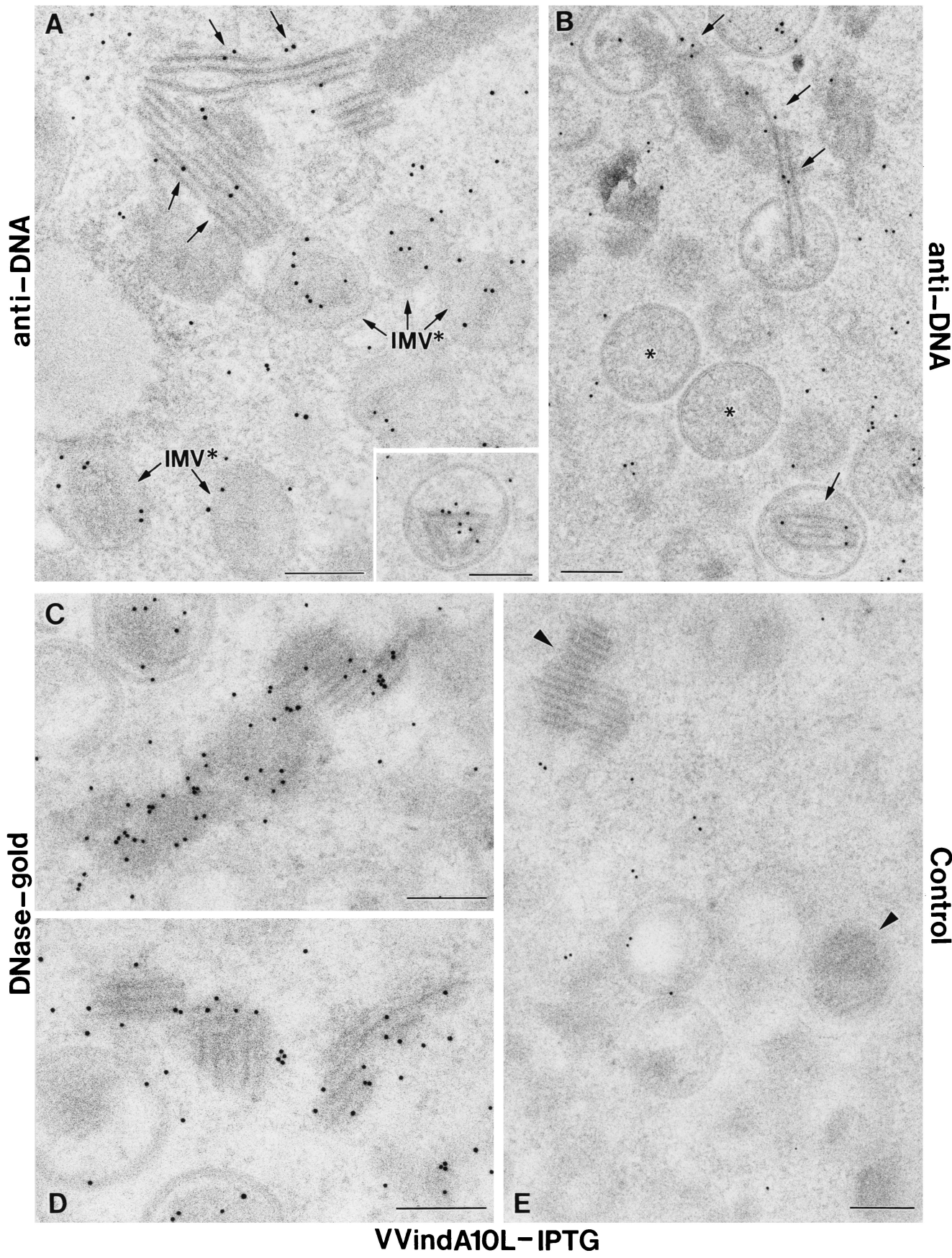
The first phenotypic characteristic of VVindA10L observed was the reduced size of viral plaques. Moreover, the mutant was essentially unable to form plaques in the absence of the inducer (the number of plaques produced without IPTG was

about 5% of the number produced in its presence). Reduced viral yields were obtained even in the presence of the inducer, which indicates that the protein is essential for viral replication and that the limited amount of this protein produced under these conditions is not enough to completely restore viral replication. Thus, addition of IPTG provides semipermissive conditions for VVindA10L growth. It has been shown for many IPTG-dependent conditional mutants that the level of expression of the *lac* operator-regulated gene is lower than WT levels. This lower level of expression of proteins which are essential for viral replication generally results in reduced viral growth; accordingly, the viral plaques produced by these conditional lethal mutants in the presence of the inducer are often smaller than WT plaques (19, 47, 64, 68, 69). Moreover, using the VOTE expression system, which allows the regulated protein to be overexpressed, it has been shown that for optimal virus production of a conditional virus that inducibly express the A5L gene coding for the 39K core protein, this protein has to be expressed to levels 10-fold higher than those found in a WT infection, suggesting a less efficient utilization of the protein by the conditional mutant (63); the same finding has been reported for other essential proteins (19, 64).

A comparative time course of protein synthesis by labeling infected cells with [³⁵S]methionine showed a clear delay of about 2 h in the onset of host protein shutoff and the concomitant appearance of viral polypeptides when cells were infected with the mutant VVindA10L both under semipermissive and nonpermissive conditions. However, the pattern of protein synthesized at 24 hpi was almost identical to that observed in VV*lacI*-infected cells, although a reduced amount of P4a was observed when infection with VVindA10L was performed in the presence of the inducer, and this protein was only barely detected when IPTG was omitted. The same was true for the 4b cleaved product. An additional difference is the presence of three still unidentified polypeptides in cells infected with VVindA10L that were absent in cultures infected with VV*lacI*. When the same cell extracts were analyzed by Western blotting with antibodies directed against different VV proteins, the most striking result was the presence of the different proteins (P4b, VP8, 39K, and 65K) in all lanes corresponding to cells infected with VVindA10L, even when extracts were from cells infected for only 2 h. The most likely interpretation is that these proteins were remnants of the input virus used to infect the monolayers. This, in turn, indicates that the inoculum used contains a high proportion of noninfectious viral particles. This hypothesis was later verified after purification of viral particles produced in the presence of IPTG (see below). In addition, this Western blot analysis confirms the reduced rate of expression and of proteolytic processing of P4a in cells infected with VVindA10L in the presence of IPTG; a similar result was obtained for P4b. The reason for the apparent reduction in the

FIG. 9. DNA localization in HeLa cells infected with VVindA10L using anti-DNA antibodies or a DNase-gold complex. Lowicryl K4M ultrathin sections of cells infected with VVindA10L in the presence (A and B) or absence (C, D, and E) of IPTG were processed for DNA detection immediately or kept at 4°C until use. Immunogold detection with a monoclonal anti-DNA antibody labeled the interior of IMV-like viral particles as well as the large dense aggregates that accumulate in the cytoplasm and the interior of IVs (A and B). (C and D) A DNase-gold conjugate of 10 nm also intensively labeled these dense structures. (E) When sections were pretreated with nonconjugated DNase (1 h at 37°C), the labeling with anti-DNA or DNase-gold was almost completely abolished. However, immunogold localization of VV proteins was not affected by DNase treatment (not shown). Bars, 200 nm.

VVindA10L+IPTG



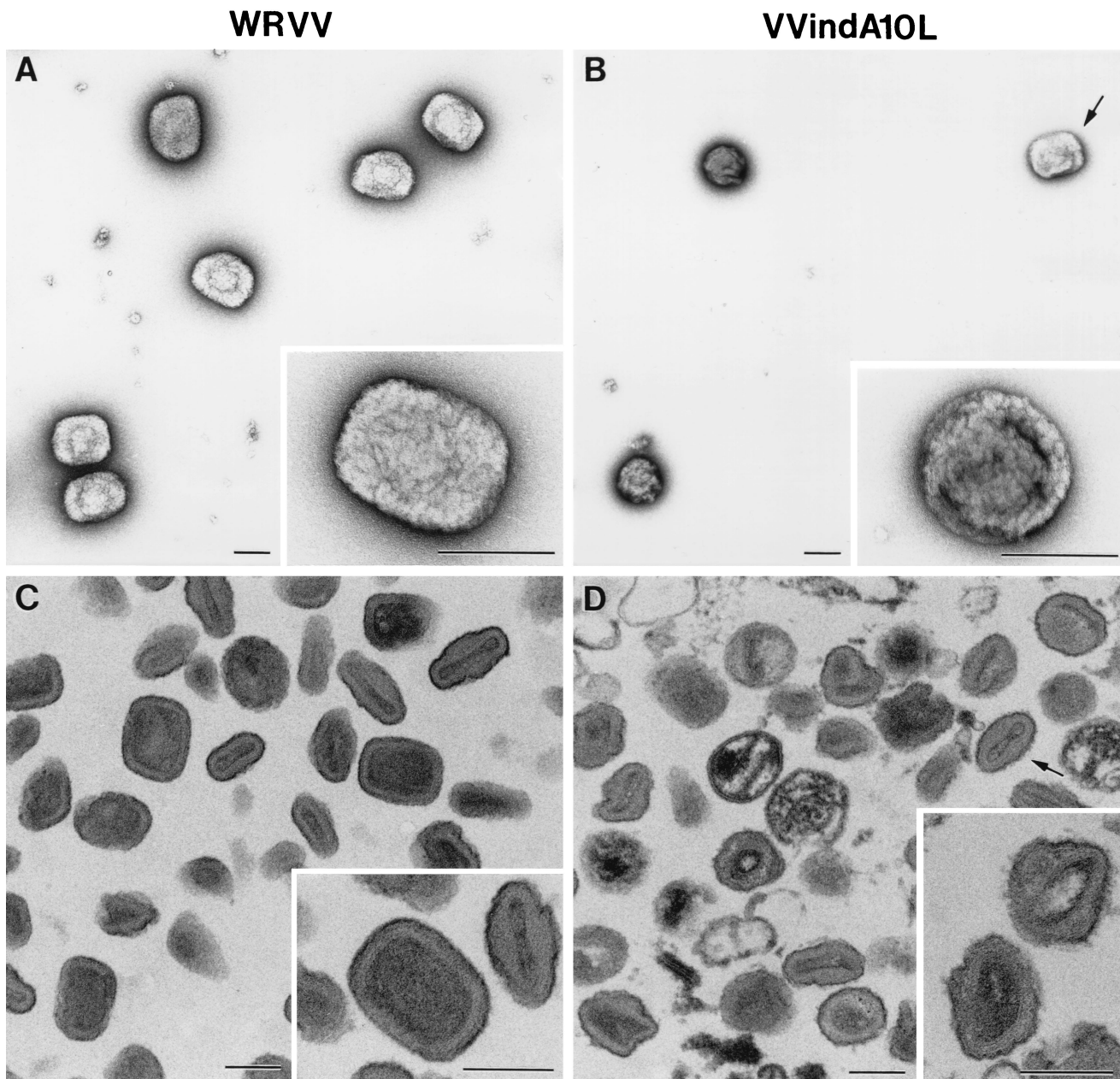


FIG. 10. Morphological characteristics of purified VVIndA10L IMVs. Suspensions of purified WR VV (A and C) and VVIndA10L (B and D) virions were processed for negative staining (A and B) or ultrathin sectioning after embedding in the epoxy resin EML-812 (C and D). (A) By negative staining, WR VV virions exhibit the characteristic brick shape, while suspensions of VVIndA10L virions (B) were mainly abnormal round particles, with a small percentage of normal, brick-shaped particles (arrow). Insets in panels A and B show representative negatively stained viral particles at higher magnification. (C and D) Ultrathin sections of the same viral suspensions show the differences in shape and internal structure of the two types of virions. VVIndA10L particles seem to be more sensitive to deformation by the process of embedding. Particles with abnormal cores and irregular contours were frequent, while a few were similar to sectioned WR VV particles (arrow). Insets in panels C and D show representative sectioned viral particles at higher magnification. Bars, 200 nm.

rate of P4b synthesis remains unknown, although a similar phenomenon was previously described for the 15K (A14L) membrane protein when synthesis of the 21K (A17L) protein was repressed (2). The extent of synthesis of VP8, 39K, and 65K proteins by 8 and 24 hpi was similar in cells infected with VVIndA10L as in those infected with VVlacI, indicating that overall, protein synthesis is not affected by the absence of P4a.

However, proteolytic processing of the core precursor VP8 seems to be also reduced in cells infected with the mutant virus, an indication that virion assembly might be blocked. On the other hand, in cells infected with VVIndA10L, synthesis of genomic DNA and processing into unit-length molecules follow the same kinetics as in cells infected with the parental VVlacI, as determined by pulsed-field analysis of viral DNA

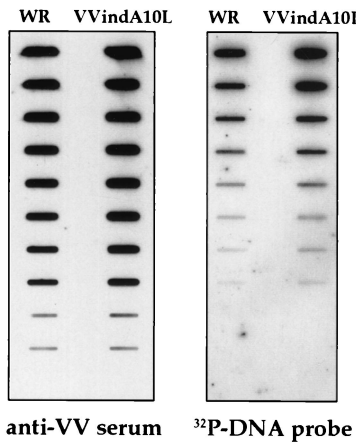


FIG. 11. Protein and DNA content of purified virus particles. Particles were purified from HeLa cells infected with WR or VVindA10L in the presence of IPTG. Aliquots were analyzed by slot blotting and reacted in Western blots against a VV polyclonal antiserum (left) or hybridized with a VV DNA probe (right).

from cells infected for different periods of time (data not shown). Thus, inhibition of viral replication should occur at a later step of the virus life cycle.

The analysis of infected cells by electron microscopy confirmed that in the absence of the P4a protein VV morphogenesis is blocked. Abnormal IVs together with very electron-dense small aggregates were abundant in the cytoplasm of cells infected with VVindA10L under nonpermissive conditions. These aggregates resemble the condensed nucleoid that can be observed inside many IVs produced in a normal infection. Electron-lucent IV-like particles devoid of viroplasmic material coexist with spherical particles filled with dense structures, with the appearance of parallel layers. No normal IVs nor IMVs were formed in the absence of P4a protein. Some IV-like particles appear either enclosing fragments of uncompleted envelopes or partially surrounded by these membrane fragments. The formation of normal VV forms is recovered in cells infected with VVindA10L in the presence of IPTG. Normal IVs enclosing viroplasmic material, IVs with dense nucleoids, and IMVs, all characteristic forms of a normal infection, are present. Aberrant IVs like those above described and abnormally rounded IMVs with an irregular electron-dense core are also seen. In addition, large regularly arranged electron-dense structures were seen between the different viral forms. Significantly, some of these dense structures are observed initiating an encapsidation-like process, suggesting that they might represent nucleoprotein complexes being taken up by the IVs. In this regard, immunogold labeling with anti-DNA antibodies and specific detection with gold-conjugated DNase confirmed the presence of DNA in these structures. The anti-DNA antibody also provide a clear signal within the IMV-like particles. Similar regularly spaced dense elements were previously observed in HeLa cells infected with a *ts* mutant (*ts6757*) generated and characterized by Dales et al. (8). They also showed the presence of numerous empty IV-like particles like those that we observe in the cytoplasm of cells infected with VVindA10L. It would be interesting to determine the genetic lesion of this *ts* mutant, which is probably in the A10L gene,

although we cannot discard the possibility that alterations in other loci may cause the same phenotypic defects. Collectively, those results show that inhibition of P4a synthesis interferes with incorporation of viroplasmic matrix by viral envelopes. An additional conclusion that can be drawn from these results is that formation of spherical viral envelopes can occur independently of viroplasm adquisition.

Inhibition of P4a synthesis appears to have no effect on the distribution of several membrane proteins like 21K, 15K, and 65K, which are localized on the envelope of the IV-like particles. Under these conditions the 14K protein, which has been described to associate with viral particles in a later stage, intermediate between IV and IMV (53), is seen in cytoplasmic accumulations. A similar distribution for the 14K protein was observed when VV morphogenesis was blocked by inhibition of synthesis of the 21K protein (44). On the other hand, the 39K core protein was present in the IV-like particles produced both in the absence and in the presence of IPTG, although in the absence of the inducer the signal was more heterogenous, with a higher amount of apparently empty IV-like particles. Moreover, from the different antibodies tested, only those raised against this protein provide a weak labeling on the regular electron-dense structures, suggesting that 39K may form part of the nucleoprotein complex. However, it remains to be determined whether antibodies to other VV proteins with DNA-binding capacity may also label these structures. Weak labeling was observed with antibodies to P4a and VP8 core proteins in IV-like particles produced in the presence of the inducer, but those produced in its absence were devoid of signal. Thus, inhibition of P4a synthesis appears to have a negative effect on the incorporation into viral particles of VP8 but not of 39K. Although we have recently shown that during normal infections 39K and P4a form a stable complex early in morphogenesis (41), the above result indicates that this interaction is not a requirement for the incorporation of the 39K protein into IVs. In this regard, it has been proposed that 39K is a membrane-associated protein, and interaction of 39K with the 21K membrane protein has been suggested (5).

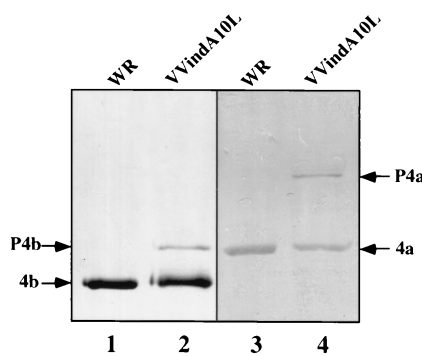


FIG. 12. Analysis by western blotting of VVindA10L and WR purified virions. Viral particles purified from cells infected with WR (lanes 1 and 3) and VVindA10L (lanes 2 and 4) in the presence of IPTG by sucrose gradient centrifugation (as described in Materials and Methods) were loaded (10 µg/lane) in 10% polyacrylamide gels. After separation by SDS-PAGE, proteins were transferred to a nitrocellulose membrane and reacted with a polyclonal antiserum against VV (lanes 1 and 2) or against the 4b core proteins (lanes 3 and 4).

Suspensions of purified WR VV and VVindA10L IMVs visualized by negative staining or sectioned after embedding in resin showed that most of VVindA10L virions are ovoid or round particles, with a small percentage of normal, brick-shaped particles. These round particles could represent abnormal particles but also intermediate maturation stages. The very low ratio between the number of infective particles and number of physical particles calculated for VVindA10L suggested that the particles of abnormal shape could be noninfectious. Adsorption of these noninfectious particles to cell monolayers would explain the high abundance of structural proteins in extracts from cells harvested at early times postinfection as mentioned before. Biochemical analysis of these particles indicated that their DNA content is normal; however, although the overall protein profile was almost undistinguishable from that displayed by WT particles, a significant difference was the presence of remnants of uncleaved P4a and P4b precursors in VVindA10L particles. This latter result favors the hypothesis that these particles are maturation intermediates. On the other hand, the few characteristic brick-shaped IMVs observed are believed to correspond to fully rescued VVindA10L particles that would account for the low infectivity of this preparation, although we cannot discard the possibility that these normal IMVs could correspond to progeny virus originated from a minor proportion of operator escape mutants that can be present in the VVindA10L virus stock and would also account for the production of the few large plaques produced in the absence of IPTG. However, we consider this possibility unlikely since characteristic IMVs were not seen in any of the many cells infected with VVindA10L under nonpermissive conditions that we have examined by electron microscopy.

As mentioned above, a question that remains to be resolved is the mechanism of DNA uptake into viral particles. Although it has not been formally proven, several studies point to the idea that the genomic DNA is packed into a nucleoprotein complex that became condensed into a nucleoid-like structure, and it is this structure that enters into unsealed IVs. The mechanism of nucleoprotein incorporation into IVs was first suggested by Morgan (31), who illustrated by electron microscopy the different steps that would result in the formation of the internal core structure. These images are not frequently seen by electron microscopy during a normal infection, suggesting that this would be a very efficient and fast process. However, certain abortive infections in which VV assembly is blocked result in the accumulation of large cytoplasmic DNA crystalloids that have the appearance of densely packed, ordered fibrils (8, 18, 31, 36, 52). Such DNA crystalloids were also seen in cells infected with a conditional mutant that inducibly expresses the A32 gene and which has been described as a DNA packaging mutant (4). Most of the viral particles produced in the absence of the A32 gene product are devoid of DNA, and thus it has been suggested that this protein is directly or indirectly involved in the process of DNA uptake. The electron-dense structures that we observe in the cytoplasm of VVindA10L-infected cells, although resembling these DNA crystalloids, are not as tightly packed, probably due to the presence of viral proteins associated to the DNA. Thus, it appears that the block in VVindA10L mutant occurs at a subsequent step, at which nucleoprotein complexes have already been formed.

In conclusion, in this report we described an inducible mutant for the core protein P4a and shown that the organization of the viral core and DNA encapsidation are impaired in the absence of the protein. The partial rescue of this mutant upon addition of IPTG may be considered advantageous since it allows visualization of intermediate stages that in a normal infection could not be observed. Further characterization of this mutant virus may provide very useful information regarding the mechanisms of packaging and incorporation of the genomic DNA into viral particles.

ACKNOWLEDGMENTS

We thank Lluís Montoliu for sharing his expertise in analyzing DNA samples by pulsed-field gel electrophoresis and Victoria Jimenez and Ana Garzón for expert technical assistance.

This work was supported by grants from the European Union (PL970064) to M.E. and from the DGICYT of Spain (PB960818) to J.L.C. J.R.R. was the recipient of a contract from the CSIC of Spain.

REFERENCES

1. Bendayan, M. 1989. The enzyme-gold cytochemical approach: a review, p. 117–147. In M. A. Hayat (ed.), *Colloidal gold: principles, methods, and applications*, vol. 2. Academic Press, Inc., San Diego, Calif.
2. Betakova, T., E. J. Wolfe, and B. Moss. 1999. Regulation of vaccinia virus morphogenesis: phosphorylation of the A14L and A17L membrane proteins and C-terminal truncation of the A17L protein are dependent on the F10 kinase. *J. Virol.* **73**:3534–3543.
3. Blasco, R., J. R. Sisler, and B. Moss. 1993. Dissociation of progeny vaccinia virus from the cell membrane is regulated by a viral envelope glycoprotein: effect of a point mutation in the lectin homology domain of the A34R gene. *J. Virol.* **67**:3319–3325.
4. Cassetti, M. C., M. Merchlinsky, E. J. Wolfe, A. S. Weisberg, and B. Moss. 1998. DNA packaging mutant: repression of the vaccinia virus A32 gene results in noninfectious DNA-deficient spherical, enveloped particles. *J. Virol.* **72**:5769–5780.
5. Cudmore, S., R. Blasco, R. Vincentelli, M. Esteban, B. Sodeik, G. Griffiths, and J. Krijnse-Locker. 1996. A vaccinia virus core protein, p39, is membrane associated. *J. Virol.* **70**:6909–6921.
6. Dales, S., and L. Siminovitch. 1961. The development of vaccinia virus in Earles L strain cells as examined by electron microscopy. *J. Biophys. Biochem. Cytol.* **10**:475–503.
7. Dales, S., and E. H. Mosbach. 1968. Vaccinia as a model for membrane biogenesis. *Virology* **35**:564–583.
8. Dales, S., V. Milovanovich, B. G. T. Pogo, S. B. Weintraub, T. Huima, S. Wilton, and G. McFadden. 1978. Biogenesis of vaccinia: isolation of conditional lethal mutants and electron microscopy characterization of their phenotypically expressed defects. *Virology* **84**:403–428.
9. Dales, S., and B. G. T. Pogo. 1981. Biology of poxviruses. *Virol. Monogr.* **18**:54–64.
10. Davison, A. J., and B. Moss. 1989. Structure of vaccinia virus late promoters. *J. Mol. Biol.* **210**:771–784.
11. DeLange, A. M. 1989. Identification of temperature-sensitive mutants of vaccinia virus that are defective in conversion of concatemeric replicative intermediates to the mature linear DNA genome. *J. Virol.* **63**:2437–2444.
12. Demkowicz, W. E., J. S. Maa, and M. Esteban. 1992. Identification and characterization of vaccinia virus genes encoding proteins that are highly antigenic in animals and are immunodominant in vaccinated humans. *J. Virol.* **66**:386–398.
13. Ericsson, M., S. Cudmore, S. Shuman, R. C. Condit, G. Griffiths, and J. K. Locker. 1995. Characterization of ts16, a temperature-sensitive mutant of vaccinia virus. *J. Virol.* **69**:7072–7086.
14. Essani, K., and S. Dales. S. 1979. Biogenesis of vaccinia: evidence for more than 100 polypeptides in the virion. *Virology* **95**:385–394.
15. Esteban, M. 1984. Defective vaccinia virus particles in interferon-treated infected cells. *Virology* **133**:220–227.
16. Falkner, F. G., and B. Moss. 1990. Transient dominant selection of recombinant vaccinia viruses. *J. Virol.* **64**:3108–3111.
17. Garcia, R., F. Almazán, J. M. Rodríguez, M. Alonso, E. Viñuela, and J. F. Rodríguez. 1995. Vectors for the genetic manipulation of African swine fever virus. *J. Biotechnol.* **40**:121–131.
18. Grimley, P. M., E. N. Rosenblum, S. J. Mims, and B. Moss. 1970. Interruption by rifampin of an early stage in vaccinia virus morphogenesis: accumulation of membranes which are precursors of virus envelopes. *J. Virol.* **6**:519–533.
19. Hu, X., L. J. Carroll, E. J. Wolfe, and B. Moss. 1996. De novo synthesis of early transcription factor 70-kilodalton subunit is required for morphogen-

- esis of vaccinia virions. *J. Virol.* **70**:7669–7677.
20. Hu, X., E. J. Wolfe, A. S. Weisberg, L. J. Carroll, and B. Moss. 1998. Repression of the A8L gene, encoding the early transcription factor 82-kilodalton subunit, inhibits morphogenesis of vaccinia virions. *J. Virol.* **72**:104–112.
 21. Ichihashi, Y., S. Matsumoto, and S. Dales. 1971. Biogenesis of poxviruses: role of A-type inclusions and host cell membranes in virus dissemination. *Virology* **46**:507–532.
 22. Johnson, G. P., S. J. Goebel, and E. Paoletti. 1993. An update on the vaccinia virus genome. *Virology* **196**:381–401.
 23. Joklik, W. K. 1962. The preparation and characteristics of highly purified radioactively labelled poxvirus. *Biochim. Biophys. Acta* **61**:290–301.
 24. Kane, E. M., and S. Shuman. 1993. Vaccinia virus morphogenesis is blocked by a temperature-sensitive mutation in the 17 gene that encodes a virion component. *J. Virol.* **67**:2689–2698.
 25. Katz, E., and B. Moss. 1970. Formation of a vaccinia virus structural polypeptide from a higher molecular weight precursor: inhibition by rifampicin. *Proc. Natl. Acad. Sci. USA* **66**:677–684.
 26. Katz, E., and B. Moss. 1970. Vaccinia virus structural polypeptide derived from a high-molecular-weight precursor: formation and integration into virus particles. *J. Virol.* **6**:717–726.
 27. Klemperer, N., J. Ward, E. Evans, and P. Traktman. 1997. The vaccinia virus II protein is essential for the assembly of mature virions. *J. Virol.* **71**:9285–9294.
 28. Leduc, E. H., and W. Benhard. 1969. Electron microscopic study of mouse liver infected by ectromelia virus. *J. Ultrastruct. Res.* **6**:466–488.
 29. Li, J., M. J. Pennington, and S. S. Broyles. 1994. Temperature-sensitive mutations in the gene encoding the small subunit of the vaccinia virus early transcription factor impair promoter binding, transcription activation, and packaging of multiple virion components. *J. Virol.* **68**:2605–2614.
 30. Merchlinsky, M., and B. Moss. 1989. Resolution of vaccinia virus DNA concatemer junctions requires late-gene expression. *J. Virol.* **63**:1595–1603.
 31. Morgan, C. 1976. The insertion of DNA into vaccinia virus. *Science* **193**:591–592.
 32. Morgan, C. 1976. Vaccinia virus reexamined: development and release. *Virology* **73**:43–58.
 33. Moss, B. 1996. Poxviridae: the viruses and their replication, p. 2637–2761. In B. N. Fields, D. M. Knipe, and P. M. Howley (ed.), *Virology*. Lippincott-Raven, Philadelphia, Pa.
 34. Moss, B., and E. N. Rosenblum. 1973. Protein cleavage and poxvirus morphogenesis: tryptic peptide analysis of core precursors accumulated by blocking assembly with rifampicin. *J. Mol. Biol.* **81**:267–269.
 35. Moyer, R. W., and R. L. Graves. 1981. The mechanism of cytoplasmic orthopoxvirus DNA replication. *Cell* **27**:391–401.
 36. Nagayra, A., B. G. Pogo, and S. Dales. 1970. Biogenesis of vaccinia: separation of early stages from maturation by means of rifampicin. *Virology* **40**:1039–1051.
 37. Payne, L. G. 1980. Significance of extracellular enveloped virus in the *in vitro* and *in vivo* dissemination of vaccinia. *J. Gen. Virol.* **50**:89–100.
 38. Ravanello, M. P., and D. E. Hruby. 1994. Conditional lethal expression of the vaccinia virus LIR myristylated protein reveals a role in virion assembly. *J. Virol.* **68**:6401–6410.
 39. Risco, C., and J. L. Carrascosa. 1999. Visualization of viral assembly in the infected cell. *Histol. Histopathol.* **14**:905–926.
 40. Risco, C., M. Muntián, L. Enjuanes, and J. L. Carrascosa. 1998. Two types of virus-related particles are found during transmissible gastroenteritis virus morphogenesis. *J. Virol.* **72**:4022–4031.
 41. Risco, C., J. R. Rodriguez, J. L. Carrascosa, M. Esteban, and D. Rodriguez. 1999. The vaccinia virus 39K protein forms a stable complex with the 4a major core protein. *Virology* **265**:375–386.
 42. Rodriguez, D., Y. Zhou, J. R. Rodriguez, D. Russell, V. Jimenez, W. T. McAllister, and M. Esteban. 1990. Regulated expression of nuclear genes by T3 RNA polymerase and lac repressor using recombinant vaccinia virus vectors. *J. Virol.* **64**:4851–4857.
 43. Rodriguez, D., M. Esteban, and J. R. Rodriguez. 1995. Vaccinia virus A17L gene product is essential for an early step in virion morphogenesis. *J. Virol.* **69**:4640–4648.
 44. Rodriguez, D., C. Risco, J. R. Rodriguez, J. L. Carrascosa, and M. Esteban. 1996. Inducible expression of vaccinia virus A17L gene provides a synchronized system to follow sorting of viral proteins during morphogenesis. *J. Virol.* **70**:7641–7653.
 45. Rodriguez, J. R., D. Rodriguez, and M. Esteban. 1992. Insertional inactivation of vaccinia virus 32K gene is associated with attenuation in mice and reduction of viral entry in polarized epithelial cells. *J. Virol.* **66**:183–189.
 46. Rodriguez, J. R., C. Risco, J. L. Carrascosa, M. Esteban, and D. Rodriguez. 1997. Characterization of early stages in vaccinia virus membrane biogenesis: implication of the 21-kDa and a newly identified 15-kDa envelope protein. *J. Virol.* **71**:1821–1833.
 47. Rodriguez, J. R., C. Risco, J. L. Carrascosa, M. Esteban, and D. Rodriguez. 1998. Vaccinia virus A14L gene product is essential for assembly and attachment of viral crescents to virosomes. *J. Virol.* **72**:1287–1296.
 48. Salanueva, I. J., J. L. Carrascosa, and C. Risco. 1999. Structural maturation of the transmissible gastroenteritis coronavirus. *J. Virol.* **73**:7952–7964.
 49. Sarov, I., and W. K. Joklik. 1972. Studies on the nature and location of the capsid polypeptides of vaccinia virions. *Virology* **50**:579–592.
 50. Schmelz, M., B. Sodeik, M. Ericsson, E. J. Wolfe, H. Shida, G. Hiller, and G. Griffiths. 1994. Assembly of vaccinia virus: the second wrapping cisterna is derived from the *trans*-Golgi network. *J. Virol.* **68**:130–147.
 51. Sekiguchi, J., and S. Shuman. 1997. Novobiocin inhibits vaccinia virus replication by blocking virus assembly. *Virology* **235**:129–137.
 52. Sodeik, B., G. Griffiths, M. Ericsson, B. Moss, and R. W. Doms. 1994. Assembly of vaccinia virus: effects of rifampin on the intracellular distribution of viral protein p65. *J. Virol.* **68**:1103–1114.
 53. Sodeik, B., S. Cudmore, M. Ericsson, M. Esteban, E. G. Niles, and G. Griffiths. 1995. Assembly of vaccinia virus: incorporation of p14 and p32 into the membrane of the intracellular mature virus. *J. Virol.* **69**:3560–3574.
 54. Van Meir, E., and R. Wittek. 1988. Fine structure of the vaccinia virus gene encoding the precursor of the major core protein 4a. *Arch. Virol.* **102**:19–27.
 55. Van Slyke, J. K., C. A. Franke, and D. E. Hruby. 1991. Proteolytic maturation of vaccinia virus core proteins: identification of a conserved motif at the N termini of the 4b and 25K virion proteins. *J. Gen. Virol.* **72**:411–416.
 56. Van Slyke, J. K., S. S. Whitehead, E. M. Wilson, and D. E. Hruby. 1991. The multistep proteolytic maturation pathway utilized by vaccinia virus P4a protein: a degenerate conserved cleavage motif within core proteins. *Virology* **183**:467–478.
 57. Van Slyke, J. K., and D. E. Hruby. 1994. Immunolocalization of vaccinia virus structural proteins during virion formation. *Virology* **198**:624–635.
 58. Whitehead, S. S., and D. E. Hruby. 1994. Differential utilization of a conserved motif for the proteolytic maturation of vaccinia virus proteins. *Virology* **200**:154–161.
 59. Whitehead, S. S., N. A. Bersani, and D. E. Hruby. 1995. Physical and molecular genetic analysis of the multistep proteolytic maturation pathway utilized by vaccinia virus P4a protein. *J. Gen. Virol.* **76**:717–721.
 60. Wilcock, D., and G. L. Smith. 1994. Vaccinia virus core protein VP8 is required for virus infectivity but not for core protein processing or for INV and EEV formation. *Virology* **202**:294–304.
 61. Wilcock, D., and G. L. Smith. 1996. Vaccinia virions lacking core protein VP8 are deficient in early transcription. *J. Virol.* **70**:934–943.
 62. Wittek, R., B. Richner, and G. Hiller. 1984. Mapping of the genes coding for the two major vaccinia virus core polypeptides. *Nucleic Acids Res.* **12**:4835–4848.
 63. Williams, O., E. J. Wolfe, A. S. Weisberg, and M. Merchlinsky. 1999. Vaccinia virus WR gene ASL is required for morphogenesis of mature virions. *J. Virol.* **73**:4590–4599.
 64. Wolfe, E. J., D. M. Moore, P. J. Peters, and B. Moss. 1996. Vaccinia virus A17L open reading frame encodes an essential component of nascent viral membranes that is required to initiate morphogenesis. *J. Virol.* **70**:2797–2808.
 65. Yang, W., S. Kao, and W. R. Bauer. 1988. Biosynthesis and post-translational cleavage of vaccinia virus structural protein VP8. *Virology* **167**:585–590.
 66. Zhang, Y., and B. Moss. 1991. Inducer-dependent conditional-lethal mutant animal viruses. *Proc. Natl. Acad. Sci. USA* **88**:1511–1515.
 67. Zhang, Y., and B. Moss. 1991. Vaccinia virus morphogenesis is interrupted when expression of the gene encoding an 11-kilodalton phosphorylated protein is prevented by the *Escherichia coli lac* repressor. *J. Virol.* **65**:6101–6110.
 68. Zhang, Y., and B. Moss. 1992. Immature viral envelope formation is interrupted at the same stage by lac operator-mediated repression of the vaccinia virus D13L gene and by the drug rifampicin. *Virology* **187**:643–653.
 69. Zhang, Y., B. Y. Ahn, and B. Moss. 1994. Targeting of a multicomponent transcription apparatus into assembling vaccinia virus particles requires RAP94, an RNA polymerase-associated protein. *J. Virol.* **68**:1360–1370.